IRSTI 31; 31:15; 31:17 https://doi.org/10.26577/ijbch.2022.v15.i2.09

F.Kh. Urakaev[1,2*], M.M. Burkitbayev[2], N.V. Khan[2]

[1] Sobolev Institute of Geology and Mineralogy, Novosibirsk, Russia
[2] Al-Farabi Kazakh National University, Almaty, Kazakhstan
*e-mail: urakaev@igm.nsc.ru

(Received 31 August 2022; received in revised form 26 September 2022; accepted 03 November 2022)

Biological activity of sulfur nanoparticles in the sulfur-dimethyl sulfoxide-water system

Abstract. For the first time a sulfur solution in dimethyl sulfoxide (DMSO) with concentration of 1.592 g/L [1] was used to prepare sulfur nanoparticles (nanosulfur). Synthesis and stabilization of colloidal sulfur particles was carried out at 298K (25 °C) by diluting the sulfur solution in DMSO with water from 10 to 1000 times. The stable sizes of nanosulfur measured by dynamic light scattering were ~ 100 nm. The results were confirmed both qualitatively and quantitatively using X-ray and electron microscopy methods. Raman spectroscopy also confirmed the presence of sulfur. The kinetics of changes in the size of sulfur nanoparticles, depending on the degree of aqueous dilution of the initial sulfur solution in DMSO was investigated. The antibacterial activity of the nanosulfur on the phytopathogenic bacterium *Erwinia amylovora* and fungus *Fusarium solani* was tested. The study of antimicrobial activity was carried out using two methods, and the results revealed the ability of the synthesized nanosulphur to suppress pathogenic microorganisms.
Keywords: dimethyl sulfoxide, sulfur solutions, dilution with water, sulfur nanoparticles, characteristics and properties, biological activity.

Introduction

It is known [1-4] that DMSO, $(CH_3)_2SO$, contains 41.04 wt.% sulfur in the bound state ($\mathbf{S_{DMSO}}$). DMSO (under standard state a liquid without color and odor, density 1.1 g/cm^3, melting point 291.7K/18.55°C, boiling point 462K/189°C) is a universal bipolar aprotic solvent [1.2] and is widely used in chemistry and technology [3-9]. DMSO mixes unlimitedly with water and organic liquids [2], and dissolves many inorganic and organic compounds [2,10], including sulfur in the form of S_8 molecules with the solubility at 298K/25°C is ≈ 1 g/L [1].

There are many methods for producing sulfur nanoparticles (nanosulfur) [11-15] that have specific properties and applications [3-9,11-21]. However, most of the proposed methods of nanosulfur preparation do not allow its antibacterial [13-15,17-21] and hydrophobic [13,16,19,21] properties to be realized on a large scale, for example, in medicine, agriculture and the building industry. Therefore, the main goal of our research is to develop a new and easy to perform multi-tonnage production of nanosulfur preparations at the place of their consumption. For this purpose we propose to use sulfur solutions in DMSO obtained at 323K/50°C and 398K/125°C in which sulfur concentrations after cooling them to 298K/25°C respectively are 1.592 and 14.152 g/l.[1] We used the method of desalting with antisolvents [22], and water was chosen as such [23,24].

In this paper, the emphasis is placed on the results of measuring the hydrodynamic diameter ***(r)*** of sulfur particles by the dynamic light scattering (DLS) method [11,25,26] using DLS data on the Z-average size [27-29]. The Z-Average size or Z-Average mean ***(d)*** used in DLS is a parameter also known as the cumulants mean. It is the primary and most stable parameter produced by the technique, which defines this mean as the "harmonic intensity averaged particle diameter". The Z-average size will only be comparable with the size measured by other techniques, if the sample is monomodal, spherical or near-spherical in shape, and monodisperse.

Another direction a research is placed on studying the biological activity of nanosulfur using standardized methods described in [30-32]. This is due to the rapidly growing interest in the large-scale application of nanosulfur as antibacterial and antifungal agent in the food industry [33,34] and as a means of improving the quality and yield of cultivated plants [35-37], to which the authors of the presented article also contributed [19,38,39].

Materials and methods

Materials. For nanosulfur preparation, the following substances were used: sulfur (especially pure, TU 6-09-2546-77, Russia); DMSO (Dimethylsulfoxid BioChemica, ≥99.5%, AppliChem GmbH, Darmstadt, Germany); water purified by the purification system Smart2Pure (Thermo Scientific, USA). To study the biological activity of nanosulfur, the following were used: Mueller-Hinton agar (MHA) (M173) (HiMedia, India); Mueller-Hinton broth (MHB) (M391) (HiMedia, India); sodium chloride (chemically pure, Mikhailovsky Reagent Plant, Russia), and purified water.

For the nanosulfur synthesis, an installation consisting of a round-bottomed flask, a reverse refrigerator, a thermometer and an oil bath was used [1,40]. To do this, 17 g of sulfur was dissolved in 1L of DMSO at 125°C. Note that the solubility of sulfur at 125°C is 52.554 g/L [1]. After dissolution of sulfur, the mixture was kept at this temperature for another 15 minutes. Next, the reaction mixture was cooled to room temperature (25°C), and the precipitate was decanted. The resulting sulfur precipitate was washed with water 2 times and dried at 70°C. The yield of the dried sulfur sample was expected to be 17−14.152=2.848 g, where 14.152 g/L is the concentration of the resulting supersaturated and stable sulfur solution in DMSO after it cools to 25°C [1]. In practice, 2.722 g was obtained, and this amount was sufficient for analytical studies.

The prepared sample was characterized with the help of different methods of analysis. To investigate the phase composition, X-ray diffraction (XRD) with MiniFlex 600 diffractometer (Rigaku Americas Corporation, USA) (copper radiation, $\lambda = 0.15405$ nm) and ICCD-PDF2 release 2016 database was used. For robustness check of the XRD, the Raman spectroscopy was conducted with Solver Spectrum (NT MDT Instruments, Russia) on the 1800/500 diffraction grating, which provides a spectral resolution of 1 cm^{-1} [9,41,42]. To determine the morphology, size and elemental composition of the grains, we conducted the SEM-EDAX analysis by using the scanning electron microscope (SEM) Quanta 200i 3D (FEI, Netherlands) equipped by the energy dispersive X-ray analysis (EDAX). For the analysis, a mixture of 1 g of sulfur sample and 40 ml of water was treated in an ultrasonic bath for 30 minutes. The sample from the surface of the resulting suspension was applied to a silicon microscope substrate.

Preparation and characterization of colloidal sulfur solutions. The size of sulfur particles in solutions was determined by DLS at an angle of 90° using a helium-neon laser with a wavelength of 633 nm and a power of 4 mW as the radiation source (Malvern-ZetasizerNano ZS90 device). To determine the morphology and size, the images of the nanosulfur were produced via JEOL JEM-1400 transmission electron microscope (TEM; JEOL; Japan) with accelerating voltage 80 kV.

Experiments on dilute solutions of sulfur in DMSO were carried out at the location of the DLS device. For example, when diluted solution of sulfur in DMSO with concentrations of 1.592 g/L by water 50 times, the aliquot 0.1 mL of the solution was poured into a test tube with 4.9 mL of water. A sample of the resulting solution was immediately taken into the device's cuvette with a volume of ≈1 mL. The first measurement of particle size was made within the two minutes, including for other degrees of dilution. The shape and sizes of the nanosulfur was determined by TEM in a similar way. The samples were also prepared directly at the microscope location by diluting the initial sulfur solution in DMSO with the same concentrations by water. Dilution was carried out by 50 times and 500 times. Then, the diluted solutions were immediately pipetted onto a collodion-coated copper grid for TEM, and after a several minutes, the nanosulfur images were obtained.

Investigation of the biological activity of nanosulfur. Microorganism strains selected for testing: *Erwinia amylovora* is a phytopathogenic bacteria that causes various plant diseases: necrosis, burns, wilting, and "wet" or "soft" rot; *Fusarium solani* is a phytopathogenic fungus that causes rot of potato tubers, tomatoes, and cereal grains. The chosen by us of their research methods are described in the recommendations [9,30-32,42].

To prepare suspensions of microorganisms of the desired concentration, a densitometer DEN−1 was used for measuring the optical density (turbidity). Suspensions of microorganisms were prepared on a saline solution of sodium chloride (0.9% NaCl). 5 mL of saline solution was introduced into the test tube, which was placed in a densitometer and the optical density was measured. First, a suspension of microorganisms was prepared with a concentration of 1.5×10^8 CFU/mL (**CFU** – colony-forming unit in microbiology) for bacteria, 2.0×10^8 CFU/mL for fungi, which corresponds to a turbidity of 0.5 units according to McFarland. Tenfold dilutions were made from these suspensions, transferring 1.0 ml of the suspension into 9.0 mL of sterile saline solution. Thus, a dilution of 1.5×10^7 CFU/mL for bacteria, and 2.0×10^7 CFU/mL for fungi was obtained.

To determine the antimicrobial activity of nanosulfur by the method of serial dilutions, a 96-well tablet was used. MHB nutrient broth of 150 μL amount was added to all the wells (from the 1st to the 24th wells). A sample of sulfur solution in DMSO was introduced at a base concentration of 1.592 g/L in the volume of 150 μL into the 1st well and serial dilutions were carried out, which were conducted by sampling a mixture of MHB (150 μL) + the test solution (150 μL) from the 1st test tube in the amount of 150 μL into the 2nd test tube, already containing 150 μL of broth. After thoroughly mixing, 150 μL of the test sample was transferred in broth from the 2nd test tube to the 3rd, which also originally contained 150 μL of broth. This procedure was repeated until the required number of dilutions was reached. Finally, 150 μL of the mixture was extracted from the last well. Thus, the following dilutions were obtained: 1:1; 1:2; 1:4; 1:8; 1:16; 1:32; 1:64; 1:128; 1:256, 1:512, 1:1024, 1:2048, 1:4096, 1:8192, 1:16384, 1:32768, 1:65536, 1:131072, 1:262144, 1:524288, 1:1048576, 1:2097152, which corresponds to the wells from the 1st to the 23rd. The 24th well served as culture control.

A 12-well tablet was used to determine the fungicidal activity of nanosulfur. MHB nutrient broth of 1 mL amount was added to all wells (from the 1st to the 12th wells). 1 mL of sulfur solution in DMSO, also with a concentration of 1.592 g/L, was introduced into the 1st well and serial dilutions were carried out, which were conducted by taking a mixture of MHB (1 mL) + the test solution (1 mL) from the 1st test tube in an amount of 1 mL into the 2nd test tube already containing 1 mL of broth. After thoroughly mixing, 1 mL of the test sample was transferred in broth from the 2nd test tube to the 3rd, which also originally contained 1 mL of broth. This procedure was repeated until the required number of dilutions was reached. In well 12, as above, only DMSO (1 mL) was added. Thus, the following dilutions were obtained: 1:1; 1:2; 1:4; 1:8; 1:16; 1:32; 1:64; 1:128; 1:256, 1:512, 1:1024, which corresponds to the wells from the 1st to the 11th, and the 12th well served as a culture control.

After a series of dilutions, 20 μL of a suspension of a test strain of a phytopathogenic bacterium at a concentration of 1.5×10^7 CFU/mL were added to the first 24 wells of the plate. In the next 12 wells, 100 μl of a suspension of the test strain of a phytopathogenic fungus was added at a concentration of 2.0×10^7 CFU/mL. Samples containing bacteria were incubated for 18-24 hours at 37±1°C, and samples containing fungi – 120 hours at 22±1°C. After the incubation time, plating was carried out on Petri dishes from MHA to determine living cells. The results were taken into account by the presence of visible growth of microorganisms on the surface of a dense nutrient medium. The minimum bactericidal / fungicidal concentration (**MBC / MFC**) was considered as the lowest concentration in the well, which suppressed the growth of microorganisms.

Determination of the antimicrobial activity of nanosulfur by the disc diffusion method (**DDM**) was also carried out by the wells method. For this purpose, wells were made with a sterile cylinder with a diameter of 6 mm at a distance of 15-20 mm from the edge of the cup and from each other. A sulfur solution in DMSO of 80 μL was added to the obtained wells. Petri dishes were pre-plated with a suspension of test strains with a density of 1.5×10^8 CFU/ml. For plating, sterile cotton swabs were used. They were immersed in a suspension of microorganism, then lightly pressed against the walls of the test tube, and shaded in three directions, while turning the cup by 60°. After seeding, the cups were placed in a thermostat for incubation for 18-24 hours at 37°C for bacteria, and for 120 hours at 22°C for fungi. The results of DDM were obtained by calculating the diameter of the growth bacteriostasis / suppression zones with an accuracy of 1 mm.

Results and discussion

XRD, Raman spectroscopy and SEM-EDAX data. Figures 1−4 show the results of a sulfur sample precipitated from its solution in DMSO with a concentration of 17 g/l at 125°C after cooling to room temperature. Figure 1 shows that the XRD lines of the sulfur sample completely correspond to its standard in the ICCD-PDF2 database, PDF Card No. 00-008-0247, in the orthorhombic, α−S_8, structure: Space Group Fddd (70). The XRD software allowed to determine the size of coherent scattering blocks (crystallite size, D = 68.6 nm) and lattice microdistortions (ε = 204%), see Figure 2.

The review article [41] shows that the α−S_8 vibrational modes at 153 cm^{-1} and 220 cm^{-1} represent, respectively, asymmetric and symmetric bending of the S−S bond. The peak at 473 cm^{-1} is associated with S−S stretching in the S_8 ring. A broad feature at ~440 cm^{-1} is present in all solid sulfur allotropes, and corresponds to S−S stretching modes. A small but distinct peak at 248 cm^{-1} characterizes intramolecular α−S_8 vibrations. External α−S_8 vibrations in the low frequency range are due to a peak at 88 cm^{-1}. These data are almost identical to the Raman spectroscopy of our sulfur sample shown in Figure 3.

According to the SEM images, for example, the sulfur sample on the tab of Figure 4 in the enlarged scale is heterogeneous in size and shape of the particles. We can see the presence of both large and small fractions of spherical, flat and other shapes, mostly, in the form of submicron agglomerates. The presence of a thin layer on top of large particles is also noticeable. The elemental and 100% content of sulfur composition of the sample on the tab is as expected, since the device could not determine the content of other minor impurities due to technical capabilities. Note that the elemental composition of sulfur in the sulfur-DMSO-water system was determined by the EDAX method for the first time.

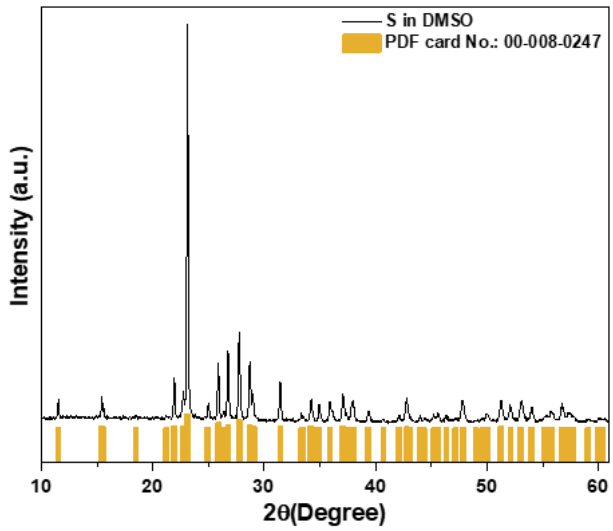

Figure 1 – X-ray phase analysis of the sulfur sample and its correspondence to the ICCD-PDF2 map.

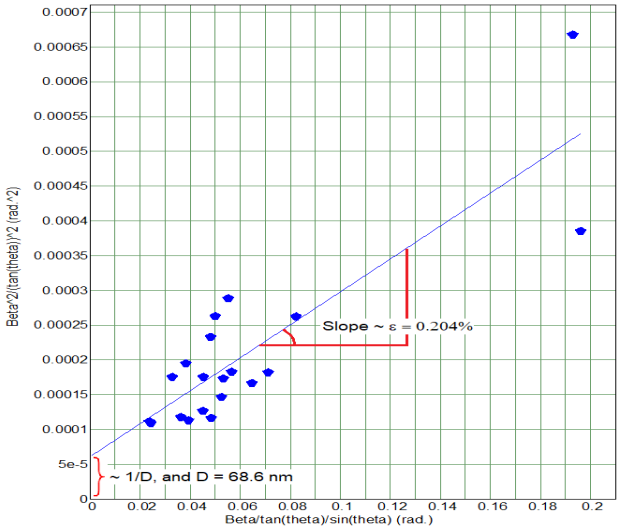

Figure 2 – Williamson-Hall plot according to the data in Figure 1.

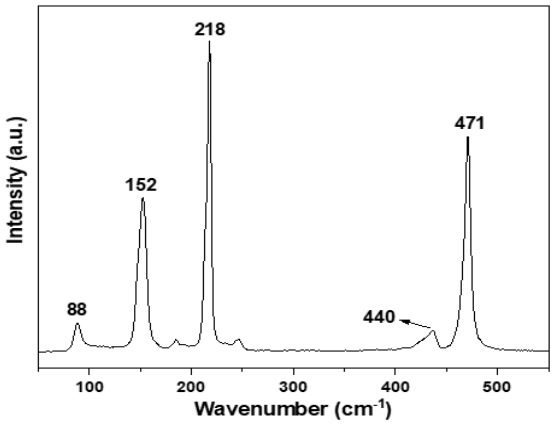

Figure 3 – Raman spectroscopy of a sulfur sample. The numbers indicate the correspondence to the data of [9,41,42].

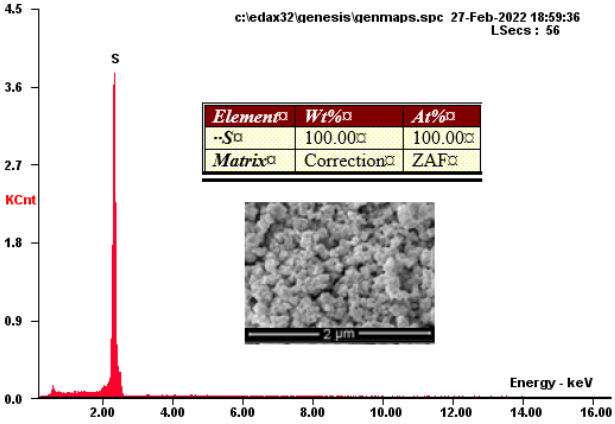

Figure 4 – SEM-EDAX of the sulfur sample. The insets show the elemental composition and SEM image of the analysis area.

DLS and TEM data. As an example, Figure 5 shows the initial (**a**) and stabilized (**b**) size distribution of sulfur particles at a 50−fold dilution with water. Similar intermediate curves of the size distribution of nanosulfur upon salting out of sulfur from its solutions in DMSO by water dilution were measured 79 times, and the option of "paired" DLS measurements was selected with the second measurement of the suspension after 103–105 s. All measurements taken are shown in **Figures S1a-S9h**

and **Table S1** in the Supplementary File. When diluted with water, only single-modal distribution functions of the type in Figure 5 were observed. **Table S1** shows the results of DLS measurements of the size and Z–Average size (r, d) of the nanosulfur and the time of stabilization of their sizes (t_s) based on the example of dilution of a sulfur solution in DMSO with the previously mentioned of 1.592 g/L for concentration. Note that dilutions of the sulfur solution in DMSO with a concentration of 14.152 g/L [1] by 1000 times are close to those for dilutions of the sulfur solution with a concentration of 1.592 g/L by 100 times. Also, see Figure 6 for TEM, dilution was carried out by 500 times and 5000 times, which is close, respectively, to dilution by 50 and 500 times of the initial sulfur solution with a concentration of 1.592 g/L used in the DLS method. Alternatively, see Figure 7 and entry nos. 7, 10 in **Table S1**. For each of them, the initial diameters of the particles (r_0, d_0) and the dynamics of their change was measured, until a little-varying stable size r_s and d_s was reached after the measurement time t_s as shown for water in Figures 5, 7. Figure 7 also shows a very good overlap of the DLS data on measuring the sizes of sulfur particles, both their hydrodynamic diameter r and Z-average diameter d. This result, obtained by diluting the initial sulfur solution in DMSO with water, allows us to assert that colloidal sulfur particles in dilute solutions has a monomodal and satisfactory narrow size distribution (close to monodisperse), and have a quasi-spherical morphology (shape).

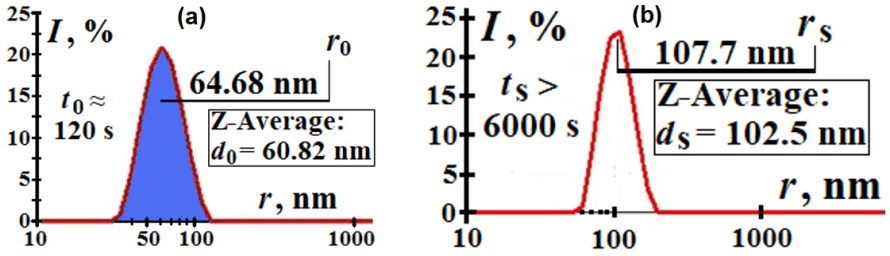

Figure 5 – Size distribution of sulfur particles, measured by DLS, after 50-fold dilution of sulfur solution in DMSO (1.592 g/L) with water: (**a**) – initial; (**b**) – after size stabilization.

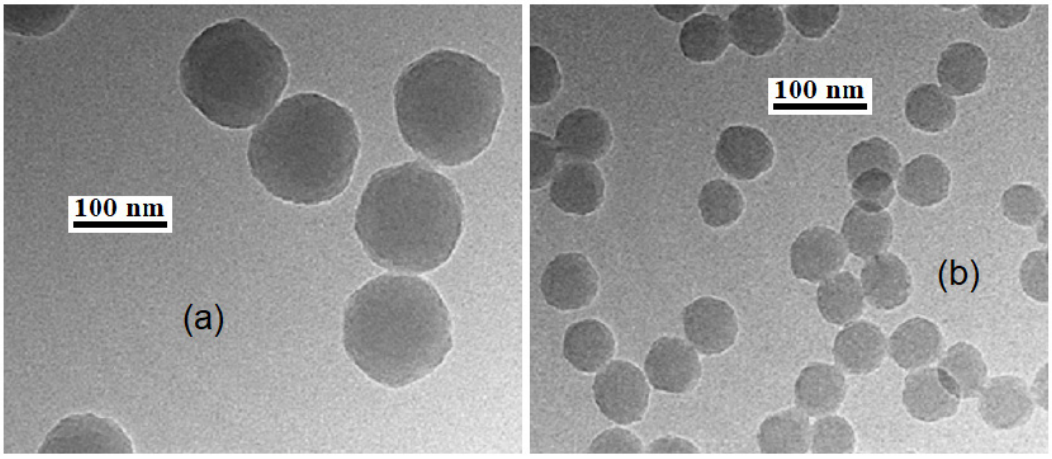

Figure 6 – TEM images of sulfur nanoparticles from sulfur solutions in DMSO diluted with water with a concentration of 14.152 g/L: (**a**) dilution degree 500 times; (**b**) – 5000 times.

Figure 6 show that all the nanoparticles have a nearly-spherical shape and the mean particle size (**a**) and (**b**) is about 60 nm and 110 nm respectively, which corresponds to results obtained from DLS experiment (match with entry nos. 6, 8 in **Table S1** of Supplementary file).

Interestingly, the stabilized dimensions of the nanosulfur depending on the degree of dilution, are

grouped by size in three and distant areas along the *r*-coordinate (Figure 7). Most likely, such groups of stable nanoparticle sizes are associated with nonmonotonic on the composition dependence and hydration nonideality in the aqueous mixtures of DMSO molecules. This is driven by the collective frame diffusion component of water reorientation, which decelerates in the water-rich regime because of the strengthened hydrogen bonds and accelerates in the water-poor regime as the hydrogen bonding network is broken into smaller aggregates [43–45]. Figure 7 also shows that the r_s and d_s values, with the exception of a 15-fold dilution, decrease as the degree of dilution increases.

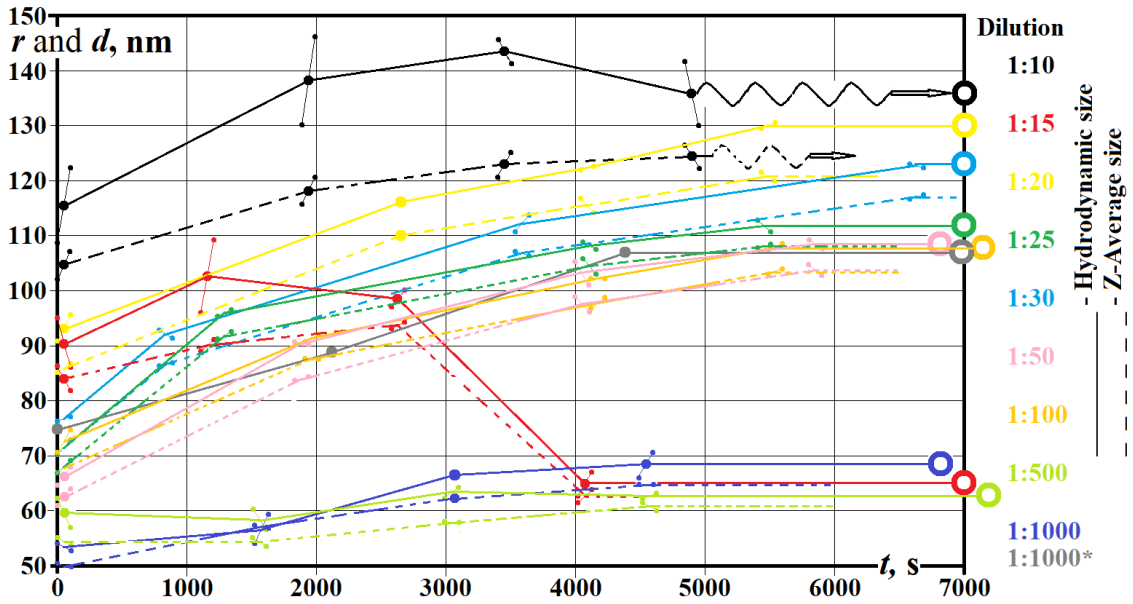

Figure 7 – Kinetics of changes in the size of sulfur nanoparticles, *r* (solid lines) and *d* (dotted lines), depending on the degree of aqueous dilution of the initial sulfur solution in DMSO with a concentration of 1.592 g/L (**Table S1**). Note: *) Solution of sulfur in DMSO with a concentration of 14.152 g/L [1] was used for dilution.

The possibility of stabilizing the size of the nanosulfur indicates that DMSO has the properties of a surfactant [46–48]. We will proceed from the obvious: the number of DMSO molecules at any degree of dilution with antisolvents exceeds the number of sulfur particles formed by orders of magnitude, and we will assume that DMSO, as a surfactant, is a micelle-forming component of the system, since it has an affinity to the surface of sulfur. In the case of the DMSO – water system, the micelle structure consists of stable complexes of these components, which, considering the hydrophobicity of sulfur particles provides maximum protection from aggregation. Therefore, the synthesis of various nanostructures with DMSO without the use of other surfactants with the participation of antisolvents is common [9,23,24,49–54].

Nanosulfur biological activity. Data of the sulfur activity in DMSO-water system against phitopathogenic microorganisms *Erwinia amylovora* and *Fusarium solani* are presented in Tables 1, 2 and in Figures 8, 9.

Table 1 – Results of antibactericidal and antifungicidal activity of a nanosulfur in DMSO-water system obtained by the method of serial dilutions.

Test-strains	MBC/MFC, µg/ml
Erwinia amylovora	1750.0
Fusarium solani	437.5

Table 2 – Results of antifungicidal and antibactericidal activity of a nanosulfur in DMSO-water system obtained by the DDM.

Test-strains	Growth suppression zone (zone diameter) M±StD, mm
Fusarium solani	18.3±2.3
Erwinia amylovora	11.7±0.6

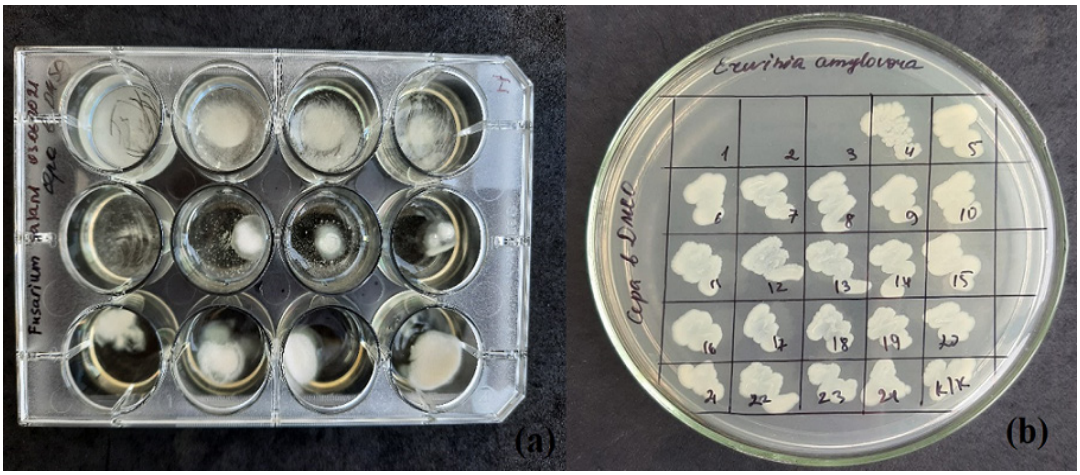

Figure 8 – Results of antimicrobial activity of a nanosulfur solution-suspension in DMSO against phytopathogenic strains (serial dilution method): (**a**) – *Fusarium solani*; (**b**) – *Erwinia amylovora*.

Our results indicate that the test sample shows antimicrobial activity against the test cultures. It has been experimentally proven that a sample of sulfur in DMSO has an antifungicidal and antibactericidal effect in dilution 1:16 (MFC value – 437.5 μg/ml) for *Fusarium solani*, and in dilution 1:4 for *Erwinia amylovora (*MBC value – 1750 μg/ml). The results of the study of a nanosulfur sample in DMSO-water system by the DDM are presented on Figure 9.

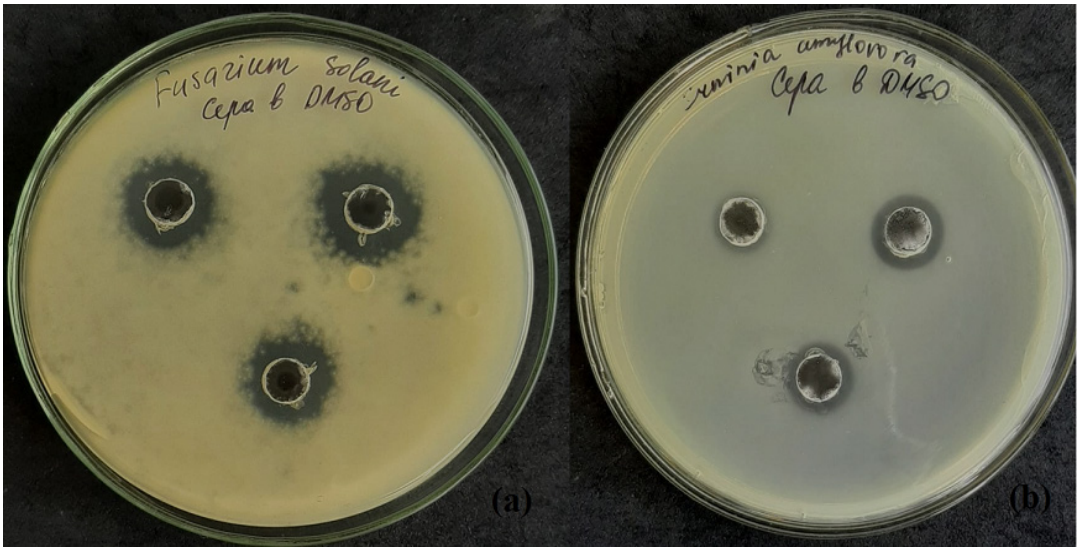

Figure 9 – Results of antimicrobial activity of colloidal nanosulfur in DMSO against phytopathogenic strains (DDM): (**a**) – *Fusarium solani*; (**b**) – *Erwinia amylovora*.

The test sample of sulfur in DMSO, when tested by the DDM, has antibacterial activity against the phytopathogenic bacterium *Erwinia amylovora*: the growth suppression zone of the phytopathogenic bacterium is 11.7±0.6 mm. With respect to the phytopathogenic fungus – *Fusarium solani*, the growth suppression zone was 18.3±2.3 mm. Thus, the results of the test sample indicate the presence of antimicrobial activity of the colloidal sulfur solution in DMSO against phytopathogenic microorganisms and the present prospects for further research.

While making conclusions, we note the presence or absence of bacteria on dense nutrient media. We count (via visual observation) the colonies that have

grown under the influence of a particular substance. A single cell, no matter what size it is (1 μm or 10 μm) gives rise to only one colony. If the substance has a bactericidal effect, we will not find a single colony. Therefore, the results are counted by the presence or absence of colony growth. At the same time, we do not count the cells visually, because it is impossible, and no further subculturing is required after obtaining the results.

Thus, we propose a new and easy method for obtaining stable colloidal solutions of sulfur. The nanosulfur in a system with water can be used for antifungal and antimicrobial treatment of cultivated plants [13-15,19-21,35-39], and can make it possible to use nanosulfur in this system for hydrophobization of porous materials [16,19,21,55,56].

Conclusions

We have demonstrated that in systems of molecular substances, dilution of sulfur solution in dimethyl sulfoxide with water makes it possible to easily synthesize and stabilize the size of sulfur nanoparticles. The average hydrodynamic diameter of sulfur nanoparticles was measured using the DLS method. DMSO-water system forms the most stable micelle-forming complexes, which, regardless of the degree of dilution (10÷1000 times) and due to the affinity of DMSO molecules to the sulfur surface, provide both the minimum size of sulfur nanoparticles (≈100 nm) and their protection from aggregation. The express method of sample preparation for TEM images, as in the case of DLS measurements, made it possible to identify quasi-spherical sulfur nanoparticles with sizes that coincide with the DLS data. Other methods used (XRD, Raman spectroscopy, and SEM-EDAX) for studying synthesized nanosulfur samples showed the presence of only orthorhombic sulfur (α−S_8), and the calculated size of sulfur crystallites by XRD was 69 nm.

The biological activity was investigated using the serial dilution method and DDM. The first method showed that the initial solution of sulfur in DMSO has bactericidal effect in dilution: 1:16 (MFC value – 437.5 μg/ml) for *Fusarium solani*; and 1:4 for *Erwinia amylovora* (MBC value – 1750 μg/ml). The tests using DDM showed that the sulfur solution in DMSO has an antibacterial effect against the phytopathogenic bacterium *Erwinia amylovora* and the growth suppression zone of the phytopathogenic bacterium is 11.7±0.6 mm. With respect to the phytopathogenic fungus – *Fusarium solani*, the growth suppression zone was 18.3±2.3 mm.

Acknowledgments

This work was supported by the Ministry of Science and Higher Education of the Republic of Kazakhstan (Grant no. AP08855868), and is done on state assignment of IGM SB RAS.

References

1. Burkitbayev M.M., Urakaev F.Kh. (2020) Temperature dependence of sulfur solubility in dimethyl sulfoxide and changes in concentration of supersaturated sulfur solutions at 25°C. *J Mol Liq*, vol. 316, pp. 113886. https://doi.org/10.1016/j.molliq.2020.113886

2. Vignes R.P. (2000) Dimethyl sulfoxide (DMSO) – a "new" clean, unique, superior solvent. American Chemical Society Annual Meeting. Washington, DC, Report (20pp). http://pedagogie.ac-limoges.fr/physique-chimie/IMG/pdf/vignes-acs.pdf

3. Tashrifi Z., Khanaposhtani M.M., Larijani B., et al. (2020) Dimethyl sulfoxide: Yesterday's solvent, today's reagent (Review). *Adv Synth Catal*, vol. 362, no. 1, pp. 65-86. https://doi.org/10.1002/adsc.201901021

4. Nakaoki T., Yamashita H. (2016) Size and weight fraction of solvent crystals in poly (vinyl alcohol) gel prepared from dimethylsulfoxide/water solution. *OJOPM*, vol. 6, pp. 86-97. http://dx.doi.org/10.4236/ojopm.2016.62009

5. Nakabayashi K., Takahashi T., Watanabe K., et al. (2017) Synthesis of sulfur-rich nanoparticles using self-assembly of amphiphilic block copolymer and a site-selective cross-linking reaction. *Polymer*, vol. 126, pp. 188-195. https://doi.org/10.1016/j.polymer.2017.08.033

6. Shi Y.-E., Zhang P., Yang D., et al. (2020) Synthesis, photoluminescence properties and sensing applications of luminescent sulfur nanodots (Review). *Chem Commun*, vol. 56, no. 75, pp. 10982-10988. https://doi.org/10.1039/D0CC04341A

7. Tan Z.L., Shi Y.L., Wei T.T., et al. Fast and facile preparation of S nanoparticles by flash nanoprecipitation for lithium-sulfur batteries. *New J Chem*, vol. 44, no. 2, pp. 466-471. https://doi.org/10.1039/C9NJ05035C

8. Jin H., Sun Y., Sun Z., et al. (2021) Zero-dimensional sulfur nanomaterials: Synthesis, modifications and applications. *Coordin Chem Rev*, vol. 438, pp. 213913.

9. Khan N., Baláž M., Burkitbayev M., et al. (2022) DMSO- mediated solvothermal synthesis of S/AgX (X = Cl, Br) microstructures and study of

their photocatalytic and biological activity, *Appl Surf Sci*, vol. 601, pp. 154122. https://doi.org/10.1016/j.apsusc.2022.154122

10. Dimethyl Sulfoxide (DMSO) Solubility data. (from November 2007, accessed at January 14, 2008) Gaylord Chemical Company, L.L.C.: Bulletin no. 102B. http://chemistry-chemists.com/N3_2011/U/DimethylSulfoxide.pdf

11. Urakaev F.Kh., Bulavchenko A.I., Uralbekov B.M., et al. (2016) Mechanochemical synthesis of colloidal sulphur particles in the $Na_2S_2O_3$–$H_2(C_4H_4O_4)$–Na_2SO_3 system. *Colloid J*+, vol. 78, no. 2, pp. 210-219. https://doi.org/10.1134/S1061933X16020150

12. Nair K.K., Kumar R., Gopal M., et al. (2018) Facile synthesis and characterization of polymer embedded catenated nanosulfur. *Mater Res Express*, vol. 5, no. 2, pp. 025007. https://doi.org/10.1088/2053-1591/aaa8bf

13. Teng Y., Zhou Q., Gao P. (2019) Applications and challenges of elemental sulfur, nanosulfur, polymeric sulfur, sulfur composites, and plasmonic nanostructures. *Crit Rev Env Sci Tec*, vol. 49, no. 24, pp. 2314-2358. https://doi.org/10.1080/10643389.2019.1609856

14. Krishnappa S., Naganna C., Rajan H.K., et al. (2021) Cytotoxic and apoptotic effects of chemogenic and biogenic nano-sulfur on human carcinoma cells: A comparative study. *ACS OMEGA*, vol. 6, no. 48, pp. 32548-32562. https://doi.org/10.1021/acsomega.1c04047

15. Kher L., Santoro D., Kelley K., et al. (2022) Effect of nanosulfur against multidrug-resistant *Staphylococcus pseudintermedius* and *Pseudomonas aeruginosa*. *Appl Microbiol Biot*, vol. 106, no. 8, pp. 3201-3213. https://doi.org/10.1007/s00253-022-11872-8

16. Urakaev F.Kh. (2011) Preparation, simulation and applications of monodisperse sulphur particles (overview). *IJCMSSE*, vol. 4, no. 1, pp. 69-86.

17. Rai M., Ingle A.P., Paralikar P. (2016) Sulfur and sulfur nanoparticles as potential antimicrobials: from traditional medicine to nanomedicine. *Expert Rev Anti-Infe*, vol. 14, no. 10, pp. 969-978. https://doi.org/10.1080/14787210.2016.1221340

18. Urakaev F.K., Abuyeva B.B., Vorobyeva N.A., et al. (2018) Formation of sulphur nanoparticles and their stabilization in the presence of water-soluble polymers. *Mendeleev Commun*, vol. 27, no. 2, pp. 161-163. https://doi.org/10.1016/j.mencom.2018.03.017

19. Massalimov I.A., Samsonov M.R., Akhmetshin B.S., et al. (2018) Coprecipitation of nanocomposites based on colloidal particles of sulfur and carbonates of alkaline-earth metals from polysulfide solutions. *Colloid J*+, vol. 80, no. 4, pp. 407-417.

20. Xu P.-F., Liu Z.-H., Duan Y.-H., et al. (2020) Microfluidic controllable synthesis of monodispersed sulfur nanoparticles with enhanced antibacterial activities. *Chem Eng J*, vol. 398, pp. 125293. https://doi.org/10.1016/j.cej.2020.125293

21. Shankar S., Jaiswal L., Rhim J.-W. (2021) New insight into sulfur nanoparticles: Synthesis and applications. *Crit Rev Env Sci Tec*, vol. 51, no. 20, pp. 2329-2356. https://doi.org/10.1080/10643389.2020.1780880

22. Poole C.F. (2020) Milestones in the development of liquid-phase extraction techniques. Liquid-Phase Extraction: A volume in Handbooks in Separation Science. Poole C.F. (editor). Elsevier, 816 p. – Ch. 1, pp. 1–44. https://doi.org/10.1016/C2018-0-00618-0

23. Zhang J., Wu P., Yang Z., et al. (2014) Preparation and properties of submicrometer-sized LLM-105 via spray-crystallization method. *Propell Explos Pyrot*, vol. 39, no. 5, pp. 653-657. https://doi.org/10.1002/prep.201300174

24. Lian B, Li Y, Zhao X, et al. (2017) Preparation and optimization of 10-hydroxycamptothecin nanocolloidal particles using antisolvent method combined with high pressure homogenization. *J Chem-NY*, vol. 2017, pp. 5752090. https://doi.org/10.1155/2017/5752090

25. Jeevanandam J. (editor), Danquah M.R. (editor). (2020) Research advances in dynamic light scattering. Series: Physics Research and Technology. New York: Nova Science Publishers, 330 p. ISBN: 978-1-53617-260-7

26. Briffa S.M., Sullivan J., Siupa A., et al. (2020) Nanoparticle tracking analysis of gold nanoparticles in aqueous media through an inter-laboratory comparison. *JoVE*, vol. 164, pp. e61741. DOI: 10.3791/61741

27. Yusof H.M., Mohamad R., Zaidan U.H., et al. (2020) Sustainable microbial cell nanofactory for zinc oxide nanoparticles production by zinc-tolerant probiotic *Lactobacillus plantarum* strain TA4. *Microb Cell Fact*, vol. 19, no. 1, pp. 10**.** https://doi.org/10.1186/s12934-020-1279-6

28. Deane O.J., Musa O.M., Fernyhough A., et al. (2020) Synthesis and characterization of waterborne pyrrolidone-functional diblock copolymer nanoparticles prepared via surfactant-free RAFT emulsion polymerization. *Macromolecules*, vol. 53, no. 4, pp. 1422-1434. https://dx.doi.org/10..1021/acs.macromol.9b02394

29. Foujdar R, Chopra H.K., Bera M.B., et al. (2021) Effect of probe ultrasonication, microwave and sunlight on biosynthesis, bioactivity and structural morphology of *Punica granatum* peel's polyphenols-based silver nanoconjugates. *Waste Biomass Valori*, vol. 12, pp. 2283-2302. https://doi.org/10.1007/s12649-020-01175-2

30. M27-A2 (2002) Reference method for broth dilution antifungal susceptibility testing of yeasts. Approved standard—second edition (www.nccls.org, ISBN 1-56238-469-4). *NCCLS*, Pennsylvania, USA, vol. 22, no. 15, 51 p. https://cupdf.com/document/m27-a2.html

32. MUC 4.12.1890-04 (2004) Methodological guidelines for determining the sensitivity of microorganisms to antibacterial drugs. Federal Center for State Sanitary and Epidemiological Supervision of the Ministry of Health of Russia, Moscow, 92 p.

30. M100-S25 (2015) Performance standards for antimicrobial susceptibility testing. *CLSI*, vol. 35, no. 3, 240 p.

33. Niranjan R., Zafar S., Lochab B., et al. (2022) Synthesis and characterization of sulfur and sulfur-selenium nanoparticles loaded on reduced graphene oxide and their antibacterial activity against gram-positive pathogens. *Nanomaterials*, vol. 12, no. 2, pp. 191. https://doi.org/10.3390/nano12020191

34. Roy S., Rhim J.W. (2022) Gelatin/cellulose nanofiber-based functional films added with mushroom-mediated sulfur nanoparticles for active packaging applications. *J Nanostruct Chem*, vol. 12, pp. 979-990. https://doi.org/10.1007/s40097-022-00484-3

35. Kaya M., Karaman R., Şener A. (2018) Effect of nano sulfur (S) application on yield and some yield properties of bread wheat. *Scientific Papers. Series A. Agronomy*, vol. LXI, no. 1, pp. 274-279. https://www.researchgate.net/publication/338253687

36. Yu Z., She M., Zheng T. et al. (2021) Impact and mechanism of sulphur-deficiency on modern wheat farming nitrogen-related sustainability and gliadin content. *Commun Biol, vol. 4*, pp. 945. https://doi.org/10.1038/s42003-021-02458-7

37. Najafi S., Razavi S.M., Khoshkam M., et al. (2022) Green synthesized of sulfur nanoparticles and its application on lettuce plants metabolic profiling. *BioNanoScience*, vol. 12, no. 1, pp. 116-127. https://doi.org/10.1007/s12668-021-00918-2

38. Burkitbayev M., Bachilova N., Kurmanbayeva M., et al. (2021) Effect of sulfur-containing agrochemicals on growth, yield, and protein content of soybeans (Glycine max (L.) Merr). *Saudi J Biol Sci*, vol. 28, no. 1, pp. 891-900. https://doi.org/10.1016/j.sjbs.2020.11.033

39. Kurmanbayeva M., Sekerova T., Tileubayeva Z., et al. (2021) Influence of new sulfur-containing fertilizers on performance of wheat yield. *Saudi J Biol Sci*., vol. 28, no. 8, pp. 4644-4655. https://doi.org/10.1016/j.sjbs.2021.04.073

40. Khan N.V. (2022) Synthesis of the S/AgBr nano/micropowder in DMSO-water system. *Chemical Bulletin of Kazakh National University*, vol. 104, no. 1, pp. 4-10. https://doi.org/https://doi.org/10.15328/cb1254

41. Nims C., Cron B., Wetherington M., et al. (2019) Low frequency Raman spectroscopy for micron-scale and in vivo characterization of elemental sulfur in microbial samples. *Sci Rep-UK*, vol. 9, no. 1, pp. 7971. https://doi.org/10.1038/s41598-019-44353-6

42. Khan N.V., Baláž M., Burkitbayev M.M., et al. (2022) Solvothermal DMSO-mediated synthesis of the S/AgI microstructures and their testing as photocatalysts and biological agents. *Int. j. biol. chem.*, vol. 15, no. 1, pp. 79-89. https://doi.org/10.26577/ijbch.2022.v15.i1.09

43. Perera A, Mazighi R. (2015) On the nature of the molecular ordering of water in aqueous DMSO mixtures. *J Chem Phys*, vol. 143, no. 15, pp. 154502. https://doi.org/10.1063/1.4933204

44. Oh K.-I., You X., Flanagan J.C., et al. (2020) Liquid-liquid phase separation produces fast H-bond dynamics in DMSO-water mixtures. *J Phys Chem Lett*, vol. 11, no. 5, pp. 1903-1908. https://doi.org/10.1021/acs.jpclett.0c00378

45. Zhang X., Wang Z., Chen Z., et al. (2020) Molecular mechanism of water reorientation dynamics in dimethyl sulfoxide aqueous mixtures. *J Phys Chem B*, vol. 124, no. 9, pp. 1806-1816. https://doi.org/10.1021/acs.jpcb.0c00717

46. Alyoussef Alkrad J., Shukla A., Mrestani Y., et al. (2016) Investigation in W/O developed microemulsions with DMSO as a cosurfactant. *Pharmazie*, vol. 71, no. 5, pp. 258-262. DOI: 10.1691/ph.2016.5122

47. Selvakumar P., Sivashanmugam P. (2020) Studies on the extraction of polyphenolic compounds from pre-consumer organic solid waste. *J Ind Eng Chem*, vol. 82, pp. 130-137. https://doi.org/10.1016/j.jiec.2019.10.004

48. Goldmann C., De Frutos M., Hill E.H., et al. (2021) Symmetry breaking in seed-mediated silver nanorod growth induced by dimethyl sulfoxide. *Chem Mater*, vol. 33, no. 8, pp. 2948-2956. https://doi.org/10.1021/acs.chemmater.1c00454

49. Cui C.-H., Li H.-H., Yu S.-H. (2010) A general approach to electrochemical deposition of high

quality free-standing noble metal (Pd, Pt, Au, Ag) sub-micron tubes composed of nanoparticles in polar aprotic solvent. *Chem Commun*, vol. 46, no. 6, pp. 940-942. https://doi.org/10.1039/B920705H

50. Nishida K., Kawasaki H. (2017) Effective removal of surface-bound cetyltrimethylammonium ions from thiol-monolayer-protected Au nanorods by treatment with dimethyl sulfoxide/citric acid. *RSC Advances*, vol. 7, no. 29, pp. 18041-18045. https://doi.org/10.1039/C7RA02179H

51. Shin S., Roh J.W., Kim H.-S., et al. (2018) Role of surfactant on thermoelectric behaviors of organic-inorganic composites. *J Appl Phys*, vol. 123, no. 20, pp. 205106. https://doi.org/10.1063/1.5033920

52. Khan N.V., Burkitbayev M.M., Urakaev F.Kh. (2019) Preparation and properties of nanocomposites in the systems S−AgI and S−Ag_2S−AgI in dimethyl sulfoxide. *Iop Conf Ser-Mat Sci*, vol. 704, no. 1, pp. 012007. https://iopscience.iop.org/article/10.1088/1757-899X/704/1/012007

53. Haidar I., Day A., Decorse P., et al. (2019) Tailoring the shape of anisotropic core-shell Au-Ag nanoparticles in dimethyl sulfoxide. *Chem Mater*, vol. 31, no. 8, pp. 2741-2749. https://doi.org/10.1021/acs.chemmater.8b04735

54. Alizadeh S., Fallah N., Nikazar M. (2020) Synthesis and characterization of direct Z-scheme CdS/TiO_2 nanocatalyst and evaluate its photodegradation efficiency in wastewater treatment systems. *Chem Pap*, vol. 74, no. 1, pp. 133-143. https://doi.org/10.1007/s11696-019-00862-2

55. Massalimov I.A., Massalimov B.I., Akhmetshin B.S., et al. (2020) Conversion of limestone-limestone mining waste by impregnation with polysulfide solutions. *Nanotechnologies in Construction*, vol. 12, no. 2, pp. 77-83. DOI: 10.15828/2075-8545-2020-12-2-77-83

56. Fediuk R., Amran Y.H.M., Mosaberpanah M.A., et al. (2020) A critical review on the properties and applications of sulfur-based concrete. *Materials (Basel)*, vol. 13, no. 21, pp. 4712. https://doi.org/10.3390/ma13214712

SUPPLEMENTARY FILE_Urakaev-et-al_IJBCh-2022 to the article: Urakaev F.Kh. [1,2*], Burkitbayev M.M.[2], Khan N.V [2] "BIOLOGICAL ACTIVITY OF SULFUR NANOPARTICLES IN THE SULFUR−DIMETHYL SULFOXIDE−WATER SYSTEM"

Solution of sulfur in DMSO with a concentration of 1.592 g/L [**S1**] was used for dilution. In the only case for measuring the size of nanosulfur in colloidal solutions, in addition to the DLS method [**S2**], see **Figures S1a−S9h**, the SALD 7101 [**S3**] device was used, see the footnote to **Table S1** of this document.

The originals of the results of measuring the sizes of nanosulfur by the DLS method.
(DMSO + Sulfur) + Water
A saturated solution of sulfur in DMSO at room temperature (1.592 g/L) is 10 times diluted with water.

Figure S1a. [DMSO + S] + Water (1/10; t = 0).

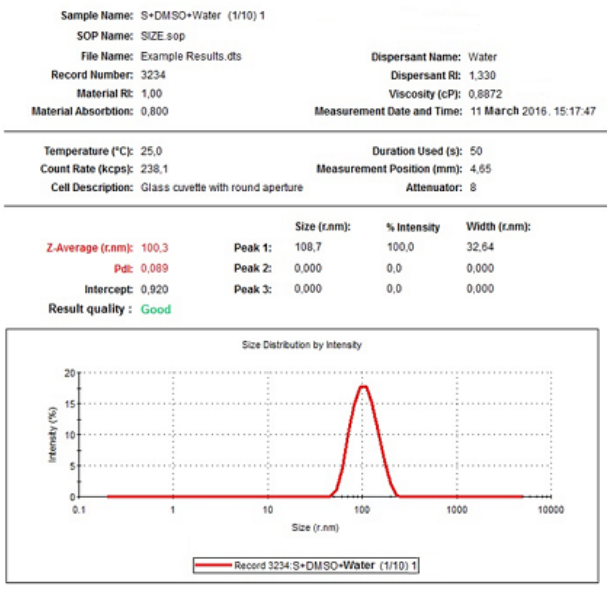

Figure S1b. [DMSO + S] + Water (1/10; t = 103 s).

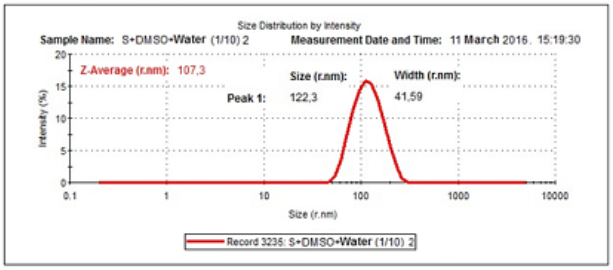

Figure S1c. [DMSO + S] + Water (1/10; t = 1886 s).

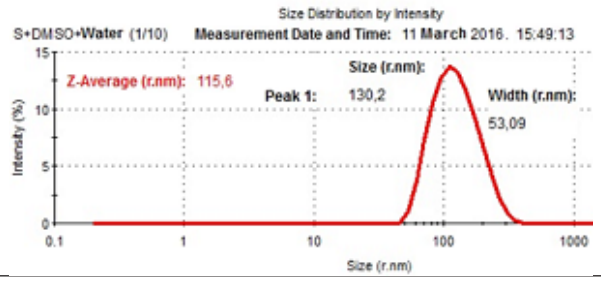

Figure S1d. [DMSO + S] + Water (1/10; t = 1989 s).

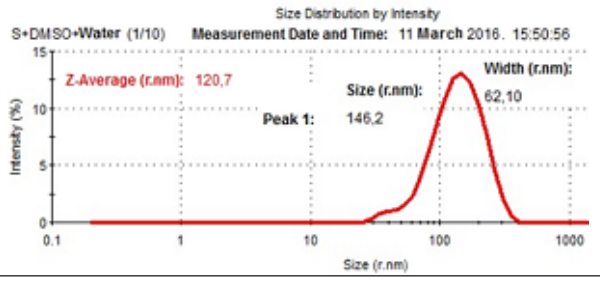

Figure S1e. [DMSO + S] + Water (1/10; t = 3404 s).

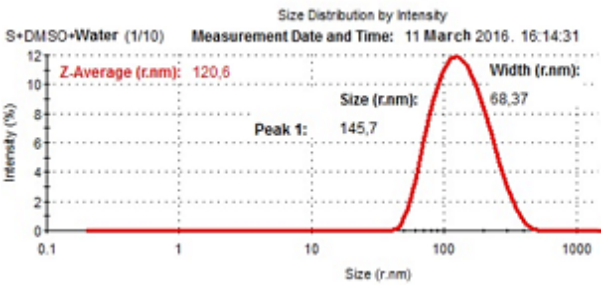

Figure S1f. [DMSO + S] + Water (1/10; t = 3508 s).

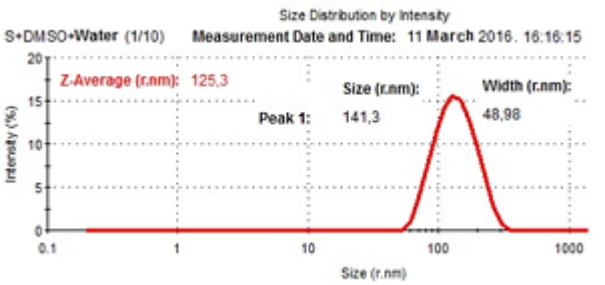

Figure S1g. [DMSO + S] + Water (1/10; t = 4845 s).

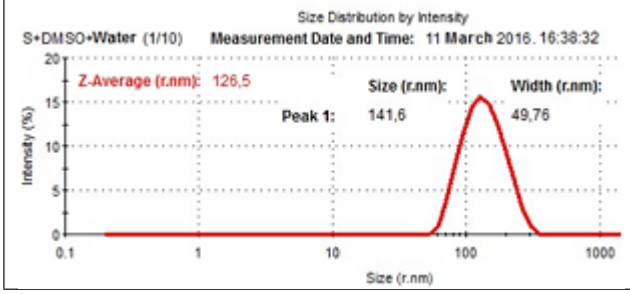

Figure S1h. [DMSO + S] + Water (1/10; t = 4949 s).

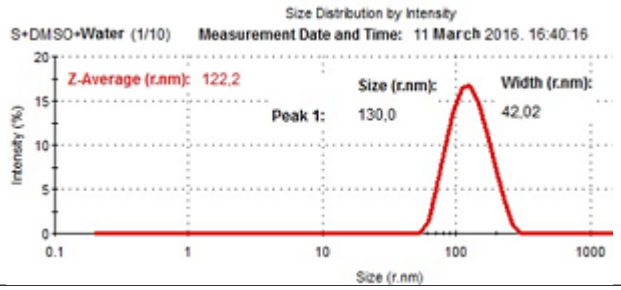

A saturated solution of sulfur in DMSO at room temperature(1.592 g/L) is 15 times diluted with water.

Figure S2a. [DMSO + S] + Water (1/15; t = 0 s).

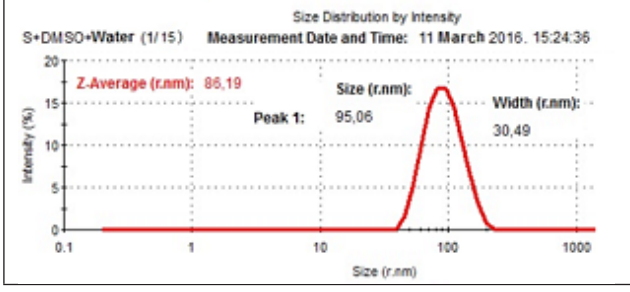

Figure S2b. [DMSO + S] + Water (1/15; t = 104 s).

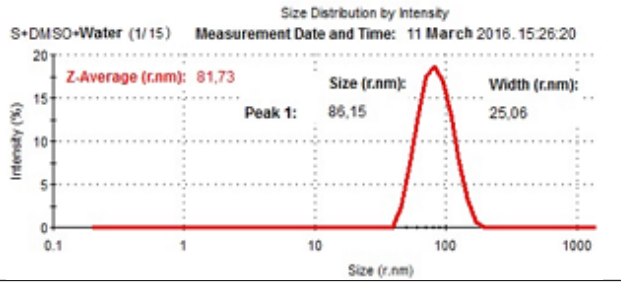

Figure S2c. [DMSO + S] + Water (1/15; t = 1106 s).

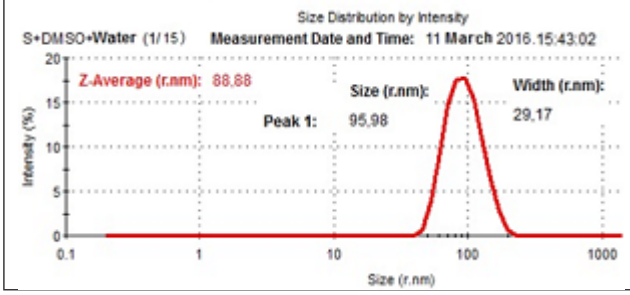

Figure S2d. [DMSO + S] + Water (1/15; t = 1210 s).

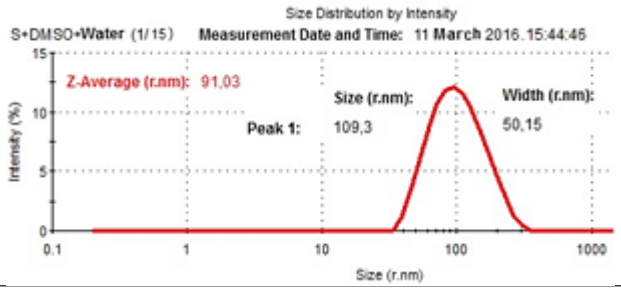

Figure S2e. [DMSO + S] + Water (1/15; t = 2578 s).

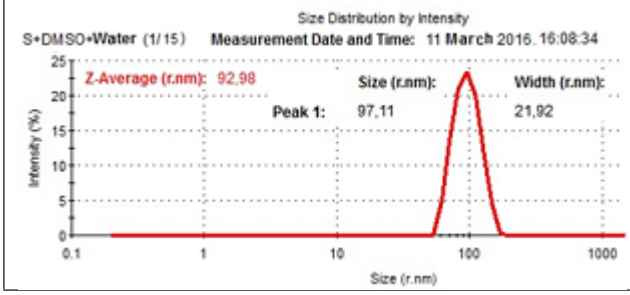

Figure S2f. [DMSO + S] + Water (1/15; t = 2682 s).

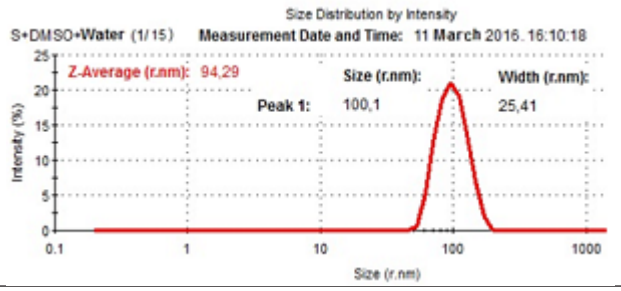

Figure S2g. [DMSO + S] + Water (1/15; t = 4018 s).

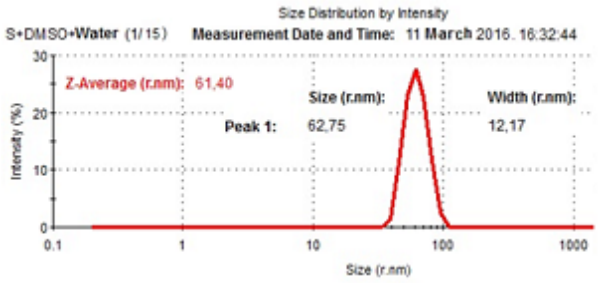

Figure S2h. [DMSO + S] + Water (1/15; t = 4121 s).

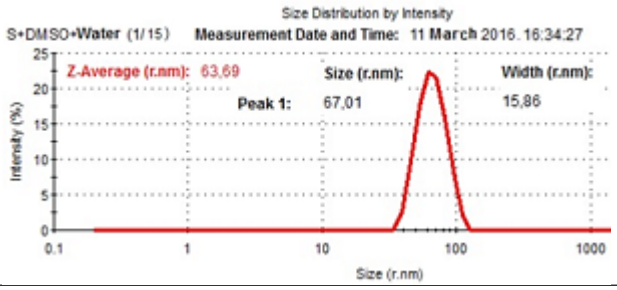

A saturated solution of sulfur in DMSO at room temperature (1.592 g/L) is 20 times diluted with water.

Figure S3a. [DMSO + S] + Water (1/20; t = 0 s).

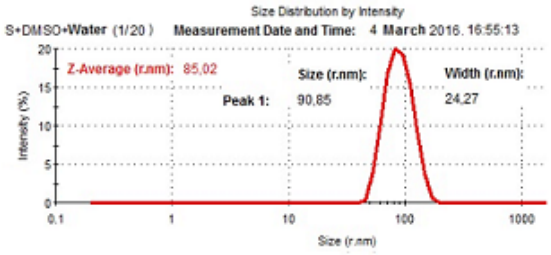

Figure S3b. [DMSO + S] + Water (1/20; t = 103 s).

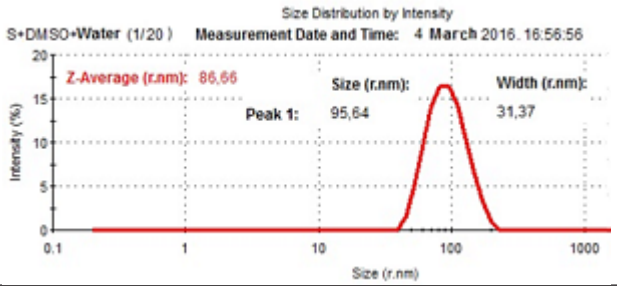

Figure S3c. [DMSO + S] + Water (1/20; t = 2652 s).

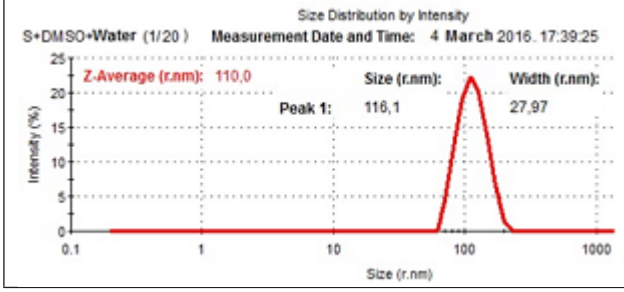

Figure S3d. [DMSO + S] + Water (1/20; t = 2756 s)?

This is "paired" with **Figure S3c** measurement for unknown reasons was not made (**missing**).

Figure S3e. [DMSO + S] + Water (1/20; t = 4037 s).

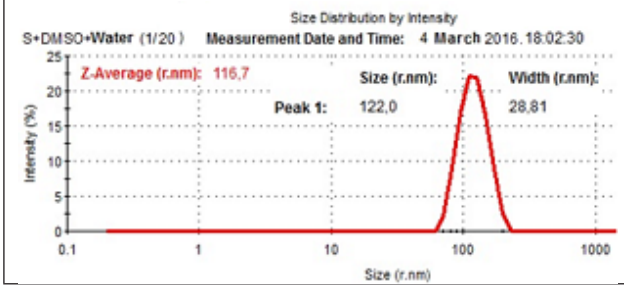

Figure S3f. [DMSO + S] + Water (1/20; t = 4141 s).

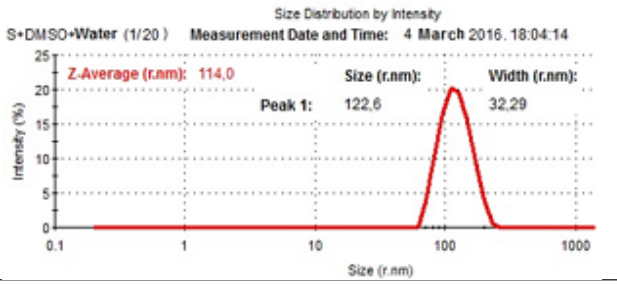

Figure S3g. [DMSO + S] + Water (1/20; t = 5435 s).

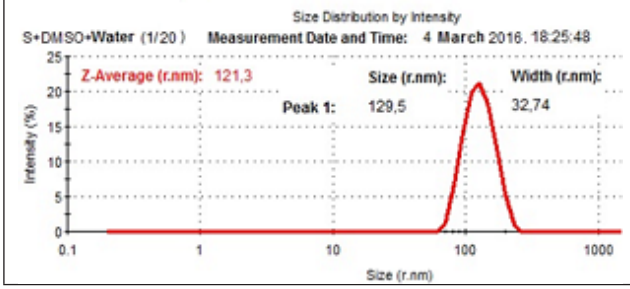

Figure S3h. [DMSO + S] + Water (1/20; t = 5539 s).

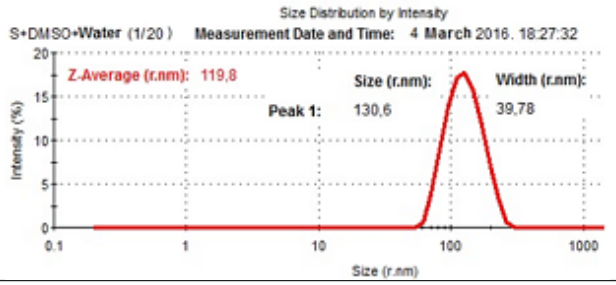

A saturated solution of sulfur in DMSO at room temperature (1.592 g/L) is 25 times diluted with water.

Figure S4a. [DMSO + S] + Water (1/25; t = 0 s).

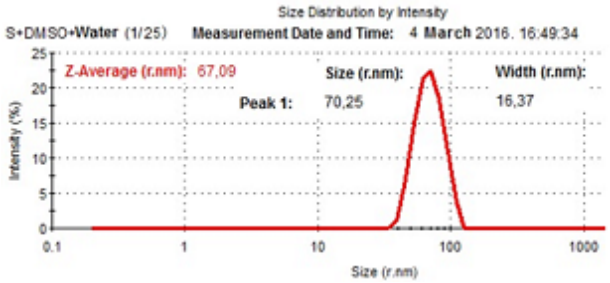

Figure S4b. [DMSO + S] + Water (1/25; t = 104 s).

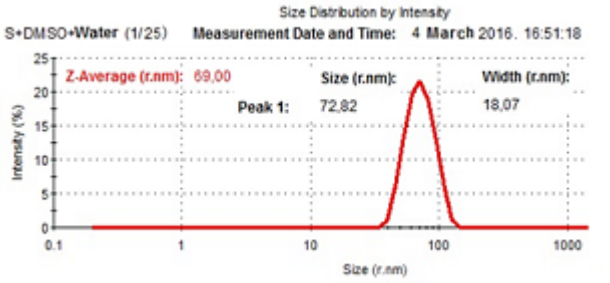

Figure S4c. [DMSO + S] + Water (1/25; t = 1236 s).

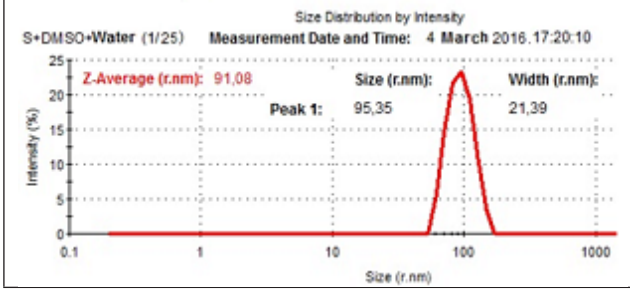

Figure S4d. [DMSO + S] + Water (1/25; t = 1340 s).

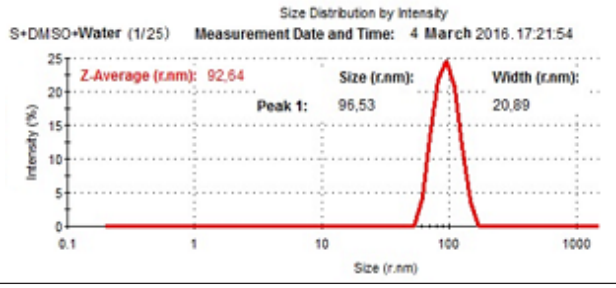

Figure S4e. [DMSO + S] + Water (1/25; t = 4054 s).

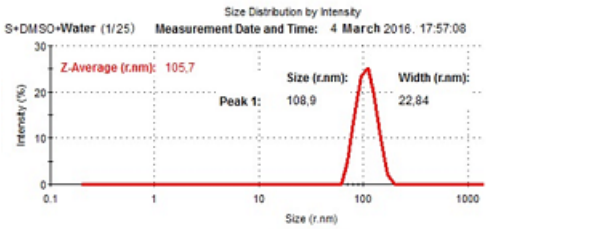

Figure S4f. [DMSO + S] + Water (1/25; t = 4157 s).

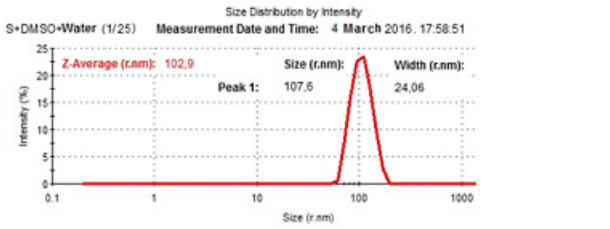

Figure S4g. [DMSO + S] + Water (1/25; t = 5405 s).

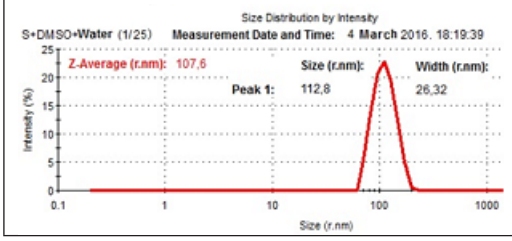

Figure S4h. [DMSO + S] + Water (1/25; t = 5508 s).

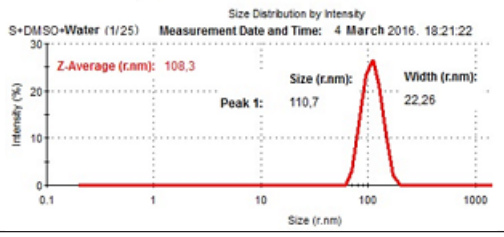

A saturated solution of sulfur in DMSO at room temperature (1.592 g/L) is 30 times diluted with water.

Figure S5a. [DMSO + S] + Water (1/30; t = 0 s).

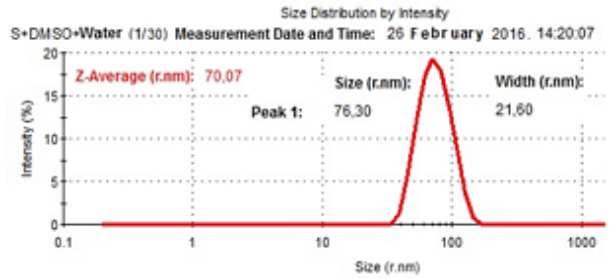

Figure S5b. [DMSO + S] + Water (1/30; t = 103 s).

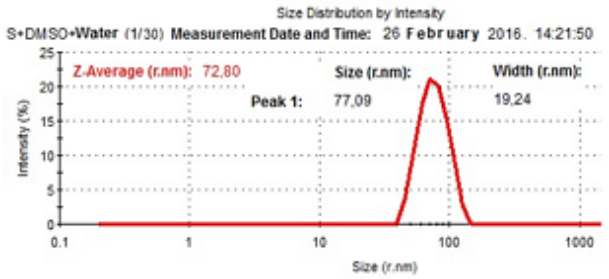

Figure S5c. [DMSO + S] + Water (1/30; t = 788 s).

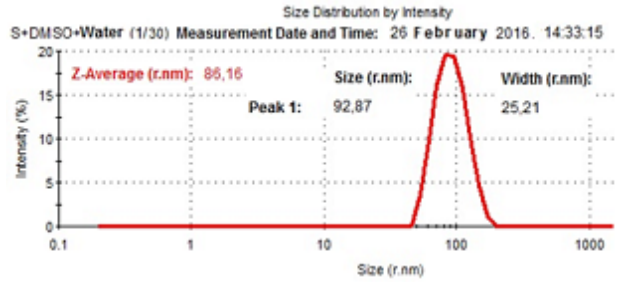

Figure S5d. [DMSO + S] + Water (1/30; t = 892 s).

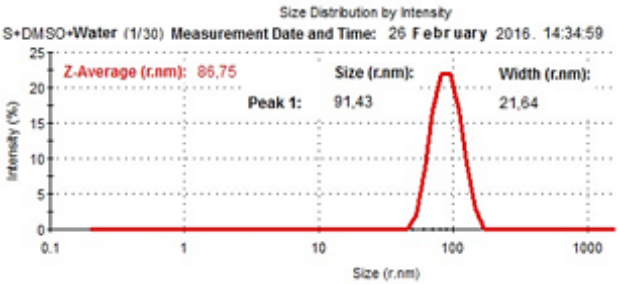

Figure S5e. [DMSO + S] + Water (1/30; t = 3535 s).

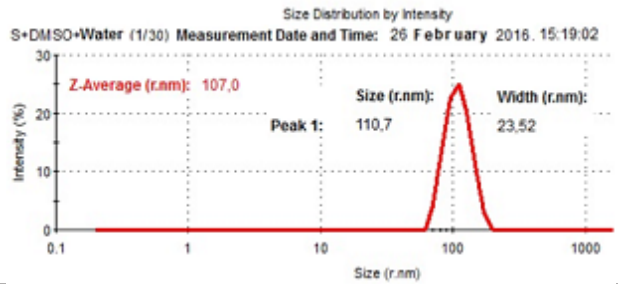

Figure S5f. [DMSO + S] + Water (1/30; t = 3639 s).

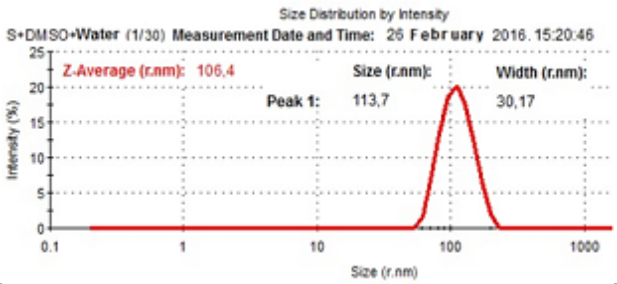

Figure S5g. [DMSO + S] + Water (1/30; t = 6579 s).

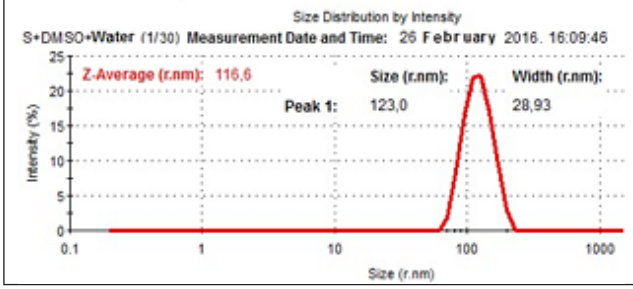

Figure S5h. [DMSO + S] + Water (1/30; t = 6683 s).

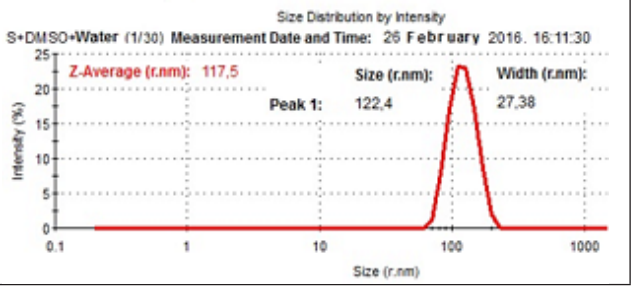

A saturated solution of sulfur in DMSO at room temperature (1.592 g/L) is 50 times diluted with water.

Figure S6a. [DMSO + S] + Water (1/50; t = 0 s).

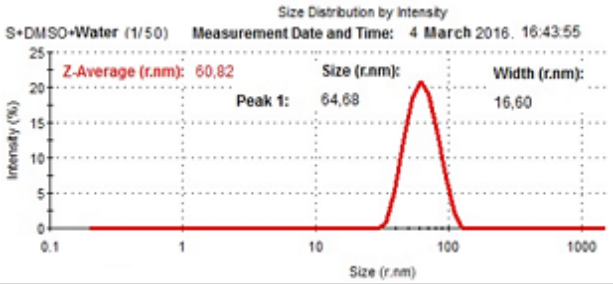

Figure S6b. [DMSO + S] + Water (1/30; t = 104 s).

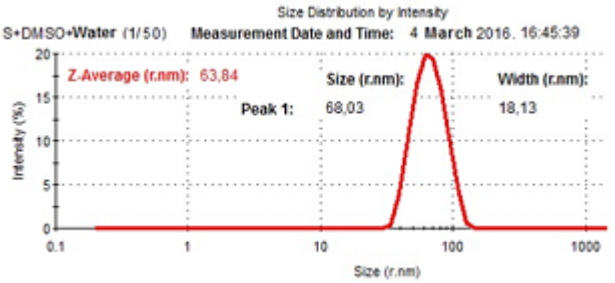

Figure S6c. [DMSO + S] + Water (1/50; t = 1833 s).

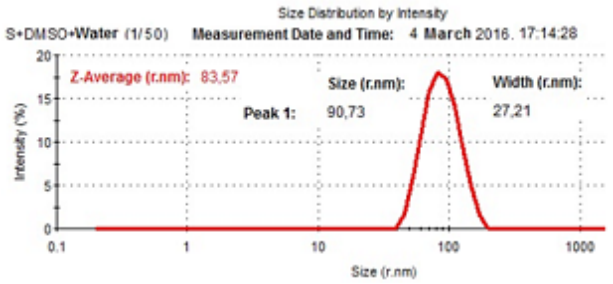

Figure S6d. [DMSO + S] + Water (1/50; t = 1936 s).

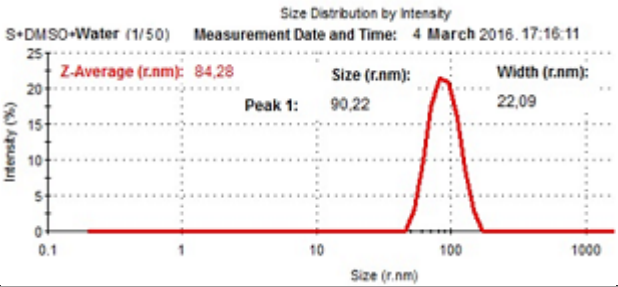

Figure S6e. [DMSO + S] + Water (1/50; t = 3995 s).

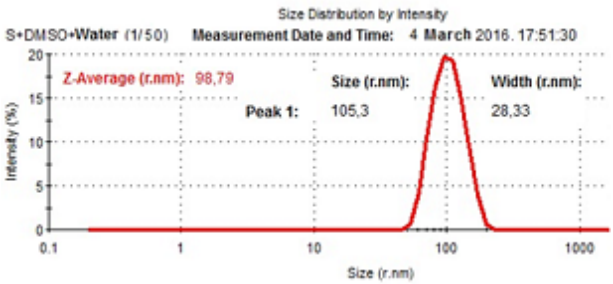

Figure S6f. [DMSO + S] + Water (1/50; t = 4099 s).

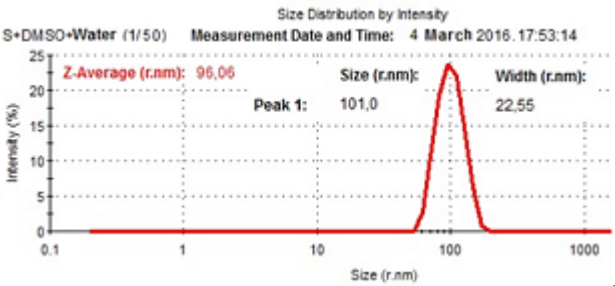

Figure S6g. [DMSO + S] + Water (1/50; t = 5408 s).

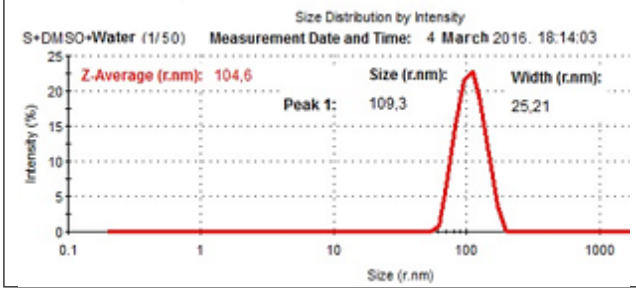

Figure S6h. [DMSO + S] + Water (1/50; t = 5513 s).

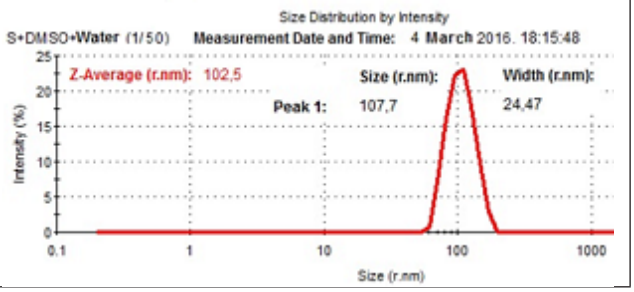

A saturated solution of sulfur in DMSO at room temperature (1.592 g/L) is 100 times diluted with water.

Figure S7a. [DMSO + S] + Water (1/100; t = 0 s).

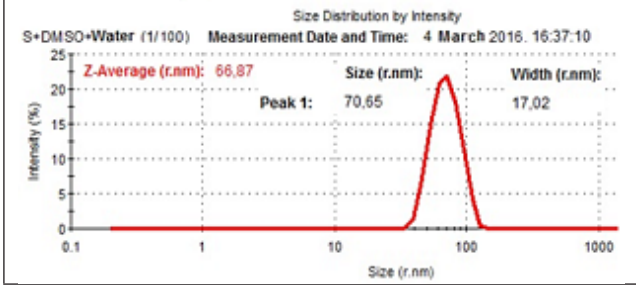

Figure S7b. [DMSO + S] + Water (1/100; t = 103 s).

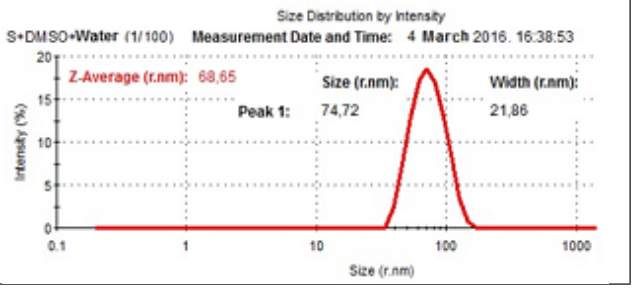

Figure S7c. [DMSO + S] + Water (1/100; t = 1911 s).

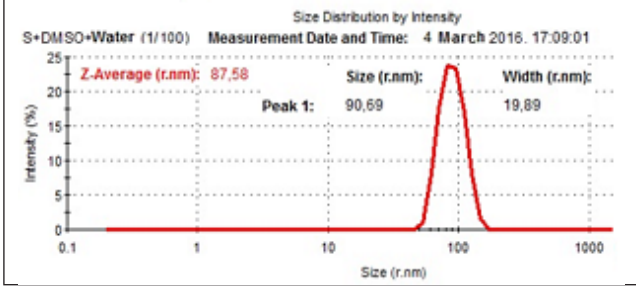

Figure S7d. [DMSO + S] + Water (1/100; t = 2015 s).

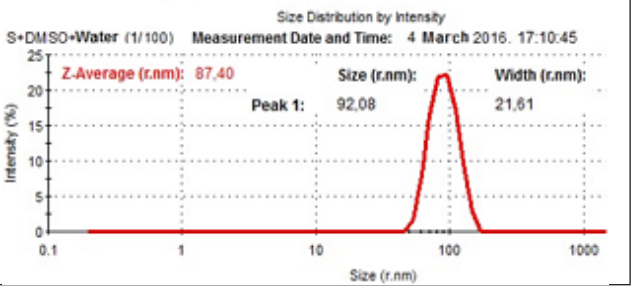

Figure S7e. [DMSO + S] + Water (1/100; t = 4120 s).

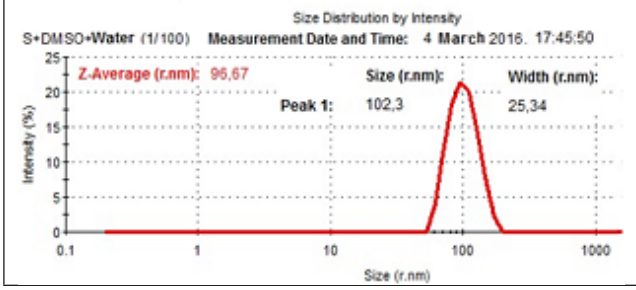

Figure S7f. [DMSO + S] + Water (1/100; t = 4224 s).

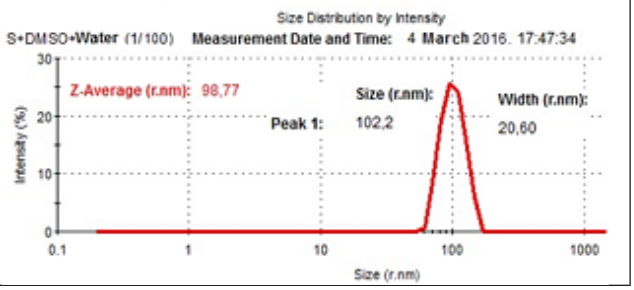

Figure S7g. [DMSO + S] + Water (1/100; t = 5491 s).

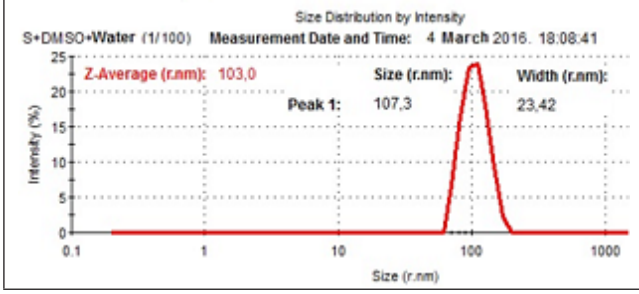

Figure S7h. [DMSO + S] + Water (1/100; t = 5595 s).

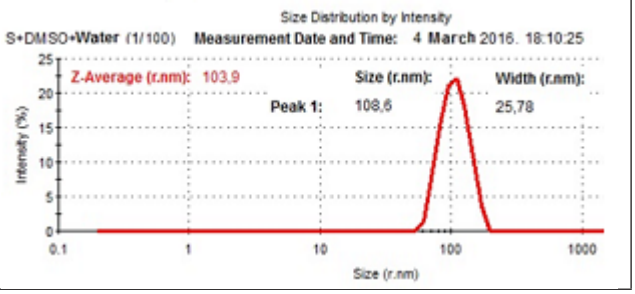

A saturated solution of sulfur in DMSO at room temperature (1.592 g/L) is 500 times diluted with water.

Figure S8a. [DMSO + S] + Water (1/500; t = 0 s).

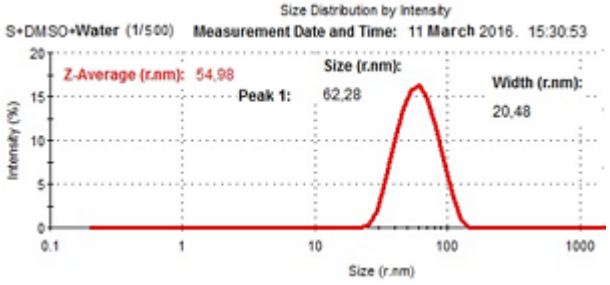

Figure S8b. [DMSO + S] + Water (1/500; t = 104 s).

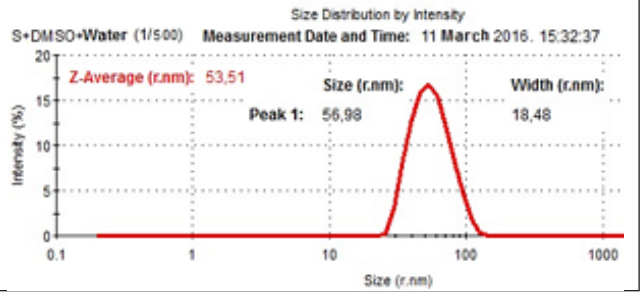

Figure S8c. [DMSO + S] + Water (1/500; t = 1509 s).

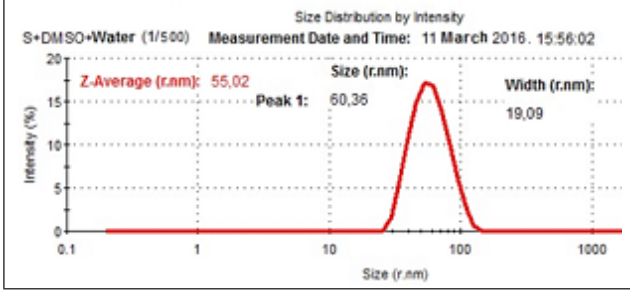

Figure S8d. [DMSO + S] + Water (1/500; t = 1613 s).

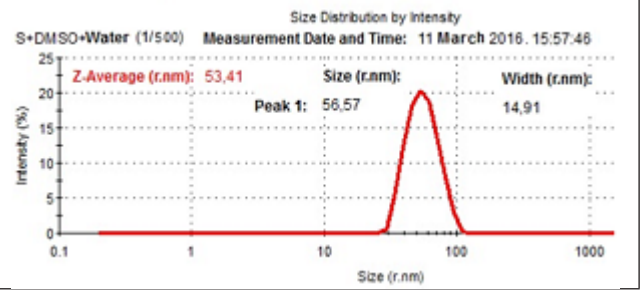

Figure S8e. [DMSO + S] + Water (1/500; t = 2991 s).

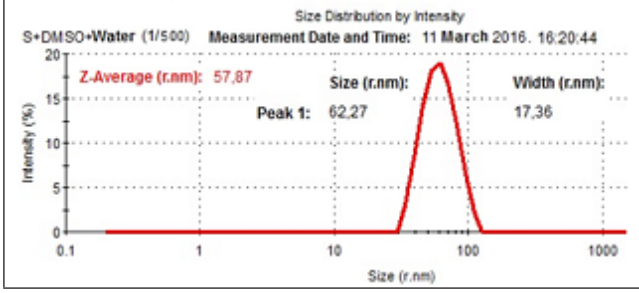

Figure S8f. [DMSO + S] + Water (1/500; t = 3094 s).

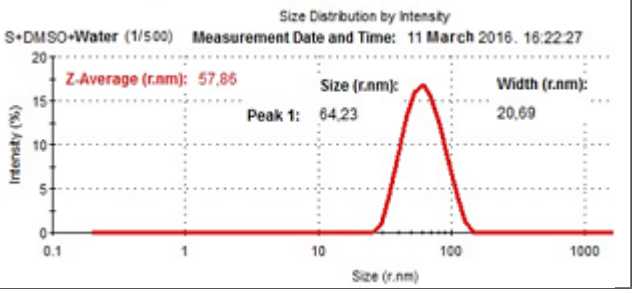

Figure S8g. [DMSO + S] + Water (1/500; t = 4518 s).

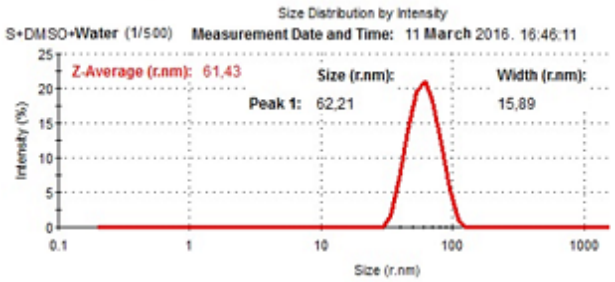

Figure S8h. [DMSO + S] + Water (1/500; t = 4622 s).

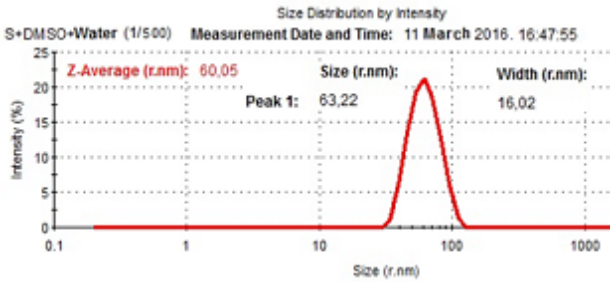

A saturated solution of sulfur in DMSO at room temperature is (1.592 g/L) 1000 times diluted with water.

Figure S9a. [DMSO + S] + Water (1/1000; t = 0 s).

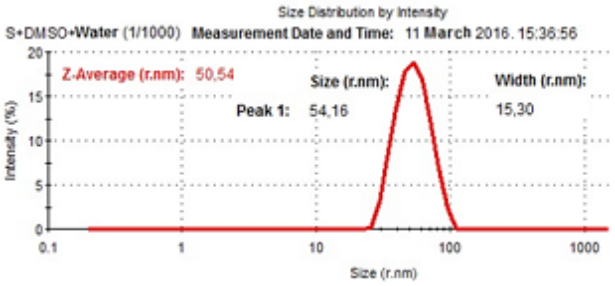

Figure S9b. [DMSO + S] + Water (1/1000; t = 105 s).

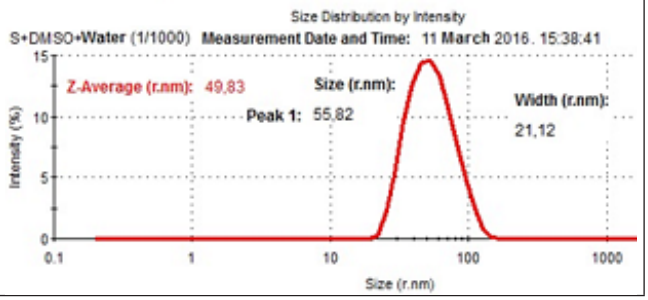

Figure S9c. [DMSO + S] + Water (1/1000; t = 1525 s).

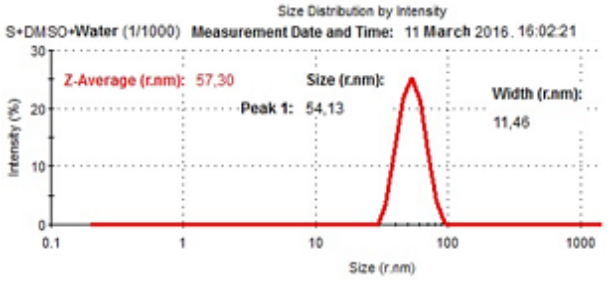

Figure S9d. [DMSO + S] + Water (1/1000; t = 1629 s).

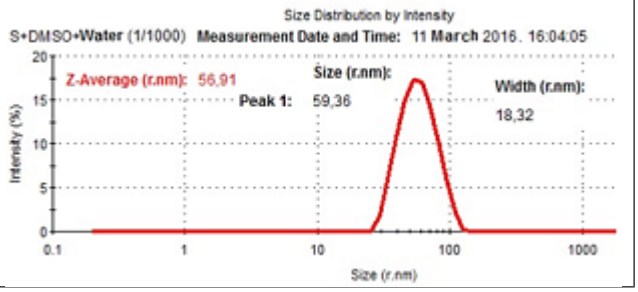

Figure S9e. [DMSO + S] + Water (1/1000; t = 3075 s).

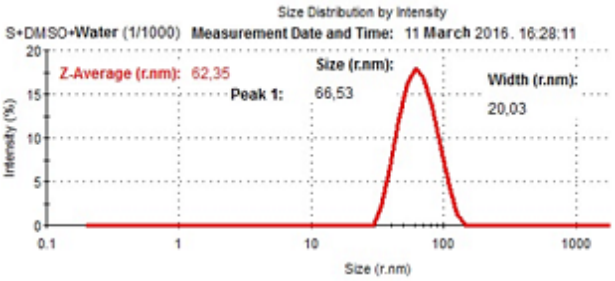

Figure S9f. [DMSO + S] + Water (1/1000; t = 3179 s)?

This is "paired" with **Figure S9e** measurement for unknown reasons was not made (**missing**).

Figure S9g. [DMSO + S] + Water (1/1000; t = 4491 s).

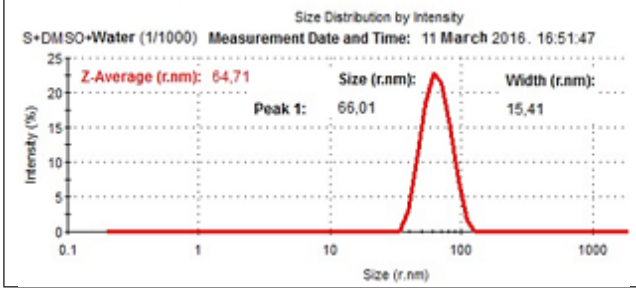

Figure S9h. [DMSO + S] + Water (1/1000; t = 4595 s).

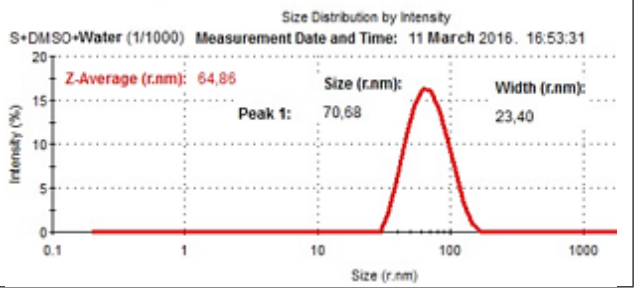

References

[**S1** or [1] in the article] Burkitbayev M.M., Urakaev F.Kh. (2020) Temperature dependence of sulfur solubility in dimethyl sulfoxide and changes in concentration of supersaturated sulfur solutions at 25°C. *Journal of Molecular Liquids*, vol. 316 (10October), pp. 113886 (5pp). https://doi.org/10.1016/j.molliq.2020.113886

[**S2** or [11]] Urakaev F.Kh., Bulavchenko A.I., Uralbekov B.M., Massalimov I.A., Tatykaev B.B., Bolatov A.K., Zharlykasimova D.N., Burkitbayev M.M. (2016) Mechanochemical synthesis of colloidal sulphur particles in the $Na_2S_2O_3$–$H_2(C_4H_4O_4)$–Na_2SO_3 system. *Colloid Journal*, vol. 78, no. 2, pp. 210-219. https://doi.org/10.1134/S1061933X16020150

[**S3** or [19]] Massalimov I.A., Samsonov M.R., Akhmetshin B.S., Mustafin A.G., Burkitbayev M.M., Shalabayev Z.S., Urakaev F.Kh. (2018) Coprecipitation of nanocomposites based on colloidal particles of sulfur and carbonates of alkaline-earth metals from polysulfide solutions. *Colloid Journal*, vol. 80, no. 4, pp. 407-417. https://doi.org/10.1134/S1061933X18040087

The above results of measuring the sizes of nanosulfur by dynamic light scattering (**DLS**) method are summarized in the following **Table S1**:

Table S1. The initial (r_0), current (r_i, i = 1, 2, 3), stabilized ($\boldsymbol{r_s}$; measurement time exceeding $\boldsymbol{t_s}$), Z−Average (d) diameters, and Width of the curve of the size distribution of sulfur nanoparticles upon dilutions of a solution of sulfur in DMSO with water, depending on the dilution degree and time t in seconds (s).

Entry no.	Dilution, times	r_0 / t_0, nm / s	r_1 / t_1, nm / s	r_2 / t_2, nm / s	r_3 / t_3, nm / s	$\boldsymbol{r_s}$, **nm;** $\boldsymbol{t_s}$, **s:**	Z-Average, d, nm:	Width, nm:
1	10	108.7/0 122.2/103	130.2/1886 146.2/1989	145.7/3404 141.3/3508	141.6/4845 130.0/4949	**136±2;** **> 5500**	100.3; 107.3, 115.6; 120.7; 120.6; 125.3; 126.5; ≈**122.2**	32.64; 41.59; 53.09; 62.10; 68.37; 48.98; 49.76; ≈**42.02**
2	15	95.06/0 86.15/104	95.98/1106 109.3/1210	97.11/2578 100.1/2682	62.75/4018 67.01/4121	**65±2;** **> 5000**	86.19; 81.73;88.88; 91.03; 92.98; 94.29; 61.40; ≈**63.69**	30.49; 25.06; 29.17; 50.15; 21.92; 25.41; 12.17; ≈**15.86**
3	20	90.85/0 95.64/103	116.1/2652 **missing**	122.0/4037 122.6/4141	129.5/5435 130.6/5539	**130±2;** **> 6000**	85.02; 86.66; 110.0; **miss.**; 116.7; 114.0; 121.3; ≈**119.8**	24.27; 31.37; 27.97; **miss.**; 28.81; 32.29; 32.74; ≈**39.78**
4	25	70.25/0 72.82/104	95.35/1236 96.53/1340	108.9/4054 107.6/4157	112.8/5405 110.7/5508	**112±2;** **> 6000**	67.09; 69.00; 91.08; 92.64;105.7; 102.9; 107.6; ≈**108.3**	16.37; 18.07; 21.39; 20.89; 22.84; 24.06; 26.32; ≈**22.26**
5	30	76.30/0 77.09/103	92.87/788 91.43/892	110.7/3535 113.7/3639	123.0/6579 122.4/6683	**123±2;** **> 7000**	70.07; 72.80; 86.16; 86.75;107.0; 106.4; 116.6; ≈**117.5**	21.60; 19.24; 25.21; 21.64; 23.52; 30.17; 28.93; ≈**27.38**
6	50	64.68/0 68.03/104	90.73/1833 90.22/19.36	105.3/39.95 101.0/40.99	109.3/5408 107.7/5513	**108±2;** **> 6000**	60.82; 63.84; 83.57; 84.28; 98.79; 96.06; 104.5; ≈**102.5**	16.60; 18.13; 27.21; 22.09; 28.33; 22.55; 25.21; ≈**24.47**
7	100	70.65/0 74.72/103	90.69/1911 92.08/1613	102.3/4120 102.2/4224	107.3/5491 108.6/5599	**108±2;** **> 6000**	66.87; 68.65; 87.58; 87.40; 96.67; 98.77; 103.0; ≈**103.9**	17.02; 21.86; 19.89; 21.61; 25.34; 20.60; 23.42; ≈**25.78**
8	500	62.28/0 56.98/104	60.36/1509 56.57/1613	62.27/2991 64.23/3094	62.21/4518 63.22/4622	**63±2;** **> 5000**	54.98; 53.51; 55.02; 53.41;57.87; 57.86; 61.43; ≈**60.05**	20.48; 18.48; 19.09; 14.91; 17.36; 20.69; 15.89; ≈**16.02**
9	1000	54.16/0 55.82/105	54.13/1525 59.36/1629	66.53/3075 **missing**	66.01/4491 70.68/4595	**68±2;** **> 5000**	50.54; 49.83; 57.30; 56.91; 62.35; **miss.**; 64.71; ≈**64.86**	15.30; 21.12; 11.46; 18.42; 20.03; **miss.**; 15.41; ≈**23.40**
10	1000 [a,b]	75±1/ 0	88±1/ 2124	100±1/ 4401	107±1/ 5702	107±2; > 6000	not given	not given

Note: [a] Solution of sulfur in DMSO with a concentration of 14.152 g/L [**S1**] was used for dilution.

[b] Measurements of the nanosulfur size were carried out on another device (SALD 7101), which excludes the option of measuring the Z-average size or Z-average value of the particle diameter (***d***), used in the DLS, therefore they are not shown in **Table S1**. The SALD 7101 analyzer [**S3**] measured particle-size distributions in a wide range of sizes from 10 nm to 300 μm in the real-time mode with a minimum time of the analysis equal to 1 s.